A Quantitative Analysis of the Unified Envelope Prediction, with Improved Data Collection Tools

By

Chris Bowen

Submitted to the graduate degree program in Bioengineering and the Graduate Faculty of the University of Kansas in partial fulfillment of the requirements for the degree of Master of Science.

<div style="text-align: right">

_____

Chair: Dr. Lorin Maletsky

_____

Dr. Elizabeth Friis

_____

Dr. Carl Luchies

</div>

Date Defended: 14 May, 2021

The thesis committee for Chris Bowen certifies that this is the approved version of the following thesis:

A Quantitative Analysis of the Unified Envelope Prediction, with Improved Data Collection Tools

_____

Chair: Dr. Lorin Maletsky

Date Approved: 14 May 2021

Abstract:

Passive laxity envelopes can provide understanding of the knee's comprehensive constraints and range of motion as well as insights not practically obtained in vivo. This research was to study variations in passive knee envelope predictions and provide recommendations for better data collection. The Experimental Joint Biomechanics Research Laboratory at the University of Kansas uses a radial basis function to generate a unified passive knee envelope and then a sequential down sampling process to study the variation in knee envelope predictions. This study had three objectives: analyze areas of high envelope variation from 13 knee predictions to better understand those variations; develop an envelope quality score to determine if the quantity and distribution of an existing data set will generate a low variation, high confidence knee envelope for a target isoload; and develop a new investigator feedback system to generate a higher quality envelope prediction. For objective 1, data sets from unified passive laxity envelopes for 13 cadaver specimens were analyzed by taking the average and standard deviation of the variations and mapping them onto the average envelope shape to compare locations of higher variation. No consistent location of variation was found, indicating the variations were not likely due to investigator instructions. This analysis did show the consistent collection of data at lower isoloads (2000 Nmm) and the under collection of data points at higher isoloads (8000-10000 Nmm), where the ligaments have a greater influence on the knee's motion. Objective 2 was to develop an envelope quality score to evaluate if an existing data set will generate a confident envelope prediction for a given isoload. Recognizing no consistent pattern in the location of variations and that the radial basis function used to interpolate data sets into a unified envelope prediction weighs data closest to the target isoload more heavily, led to the analysis of a given data set relative to a target isoload. Based on these findings, an envelope quality scoring calculation was developed based on the distance, quantity, and distribution of data points relative to a given isoload. The data points were totaled if points were located within the Euclidean norm distance of 0.25 from each vertex in the envelope isoload surface. The resulting score helps investigators assess if an existing data set will produce an envelope prediction with less variation and greater confidence. Objective 3 was to create a new investigator feedback system based on tailoring data collection to the RBF process and providing real time guidance for data collection. This was done using a MATLAB program that calculates how collected data are distributed around the target isoload and graphically displays data points on a color-coded isoload and an RBF prediction feed for the developing envelope displayed on the feedback screen. Color coding shows the investigator areas where sufficient data around the target isoload has been collected, and areas where additional data points are still needed. Displaying this in near real time (updated in 1 second increments) gives the investigator opportunity to make needed adjustments during initial data collection. Eliminating possible sources of data collection inaccuracies like manipulation motions, differences in knee kinematics or demographics could further improve envelopes. Future work might determine best isoloads for specific studies, add the envelope quality score to the investigator feedback screen, or allow the investigator to change the target isoload as they collect data. Finally, increasing program efficiency for quicker computation may increase its potential use in clinical settings.

Contents

List of Abbreviations:

ACL   Anterior Cruciate Ligament

AP   Anterior-Posterior

EJBRL Experimental Joint Biomechanics Research Laboratory

IE   Internal-External

IRED   Infrared Emitting Diode

LCL   Lateral Collateral Ligament

MCL   Medial Collateral Ligament

PCL   Posterior Cruciate Ligament

RBF   Radial Basis Function

SDSP   Sequential Down Sampling Process

SI   Superior-Inferior

TKA   Total Knee Arthroplasty

VV   Varus-Valgus

Chapter 1: Introduction

Knee motion is dictated by the different anatomical structures that constrain it [1]. The articular geometry, the ligaments (anterior cruciate ligament or ACL, posterior cruciate ligament or PCL, medial collateral ligament or MCL, lateral collateral ligament or LCL), other soft tissues, external loads, and muscle activation all help determine the knee's range of motion. Researchers and physicians evaluate the laxity of a knee to diagnose its function so that interventions can be optimally designed or performed on it. For researchers, one of the best ways to do this is using passive laxity envelope testing, where the muscle activation is limited by externally manipulating the joint [2]. In a research lab setting, investigators record the primary motion of the knee, flexion extension, along with several other motions such as varus/valgus (VV), internal/external (IE), anterior/posterior (AP), and superior/inferior (SI). In a clinical setting, doctors and surgeons use clinical laxity evaluations, such as the Lachman's Test and Anterior Drawer Test to determine and diagnose if there is a damaged ligament [3, 4]. The clinician or surgeon uses the results from these research and clinical knee laxity studies, along with other considerations like the patient's general health, age, bone health, and activity level to provide the most appropriate treatment for that patient. A wide range of treatment options are available, ranging from physical rehabilitation to total knee arthroplasty (TKA) which may involve implants, which have a reported life span of 10-20 years depending on the success of restoring the proper alignment and balance of the knee [5]. All of these considerations lead clinicians to seek the best tests and understanding of the constraints and range of motion of a patient's knee.

Passive laxity studies performed on cadaver specimens give a prediction of the knee's complete range of motion, considering all combined constraints rather than just specific ligament

constraints. By using cadaver knees before and after a total knee replacement, researchers can study how the alterations from a surgeon affect the passive motion of the knee. Research methods that evaluate the passive laxity of a cadaver knee utilize a motion capture system along with a load cell to accurately measure the force and displacement on a cadaver specimen. These data can then be given to manufacturers to help further improve the implant design or alter the design if a problem is seen. The Experimental Joint Biomechanics Research Laboratory (EJBRL) at the University of Kansas uses a protocol that gathers a point cloud of data as the knee travels through its range of motion. These data are then processed with a Radial Basis Function (RBF) which can interpolate the data to generate a prediction of the entire envelope [5]. The RBF is a network processing method that gives different weights to various data points based on how much data are collected around specific torques. Using a method called the sequential down sampling process (SDSP), it can generate several predictions and compare the prediction of each point, giving a relative confidence in the prediction.

The 3 objectives of this study were to:

1. Develop a better understanding of the cause of prediction variations.

2. Develop a new envelope quality score calculation to determine if the quantity and distribution of an existing data set will generate a high-quality knee envelope for a target isoload.

3. Develop a new investigator feedback system for more efficient and effective data collection to generate a higher quality envelope prediction.

Chapter 2: Background

Anatomy and Physiology

Fig. 1 is a representation of the knee components and their relationship to each other. The diagram shows the anterior and posterior view of the same knee. The motion of the knee is dictated by different anatomical constraints [1]. To understand how the knee moves throughout daily activities, it is important to understand how the anatomical constraints work together. The ACL connects to the femur between the condyles of the femur and the intercondylar eminence of the tibia. The function of the ACL is to constrain the tibia from translating anteriorly and provide IE constraint [6]. It has also been shown that the tension that occurs in the ACL is dependent on the flexion angle. Markolf et al. found that ACL deficient subjects had an increase in IE laxity [7]. The PCL connects the posterior intercondylar area and inserts into the lateral surface of the medial femoral condyle. With this connection, it creates a crossing pattern with the ACL causing some binding to occur when the knee undergoes a rotational force [8, 9]. It constrains the tibia from translating in the posterior direction across all angles of flexion extension [10, 11]. The MCL has a primary role of valgus resistance and minor roles in IE rotation and anterior translation [12]. The LCL gives resistance in the varus rotation, however the structure provides less constraint after 30° flexion [13].

The articular geometry also influences the kinematics, limiting flexion extension and offering physical surfaces that constrain some of the motion [14]. The combination of these structures and the articular geometry of the human knee work together throughout flexion extension to provide stability during daily motions.

Clinical Relevance

The knee undergoes three to four times the body weight of force during everyday activities, even more during more intensive activities [14]. Knee injuries are common and ACL reconstructive surgeries have increased 12 fold the past 20 years as reported by Abram et al. [15]. Because knee injuries continue to increase and surgical solutions and implants last only 10-20 years [14], clinicians need improved diagnostic tools like passive laxity knee envelope predictions to make further improvement in implants, surgical techniques, and other treatments.

Two clinical laxity tests, the Anterior Drawer and Lachman tests, were developed to determine if the ACL has been damaged. The Anterior Drawer test requires the patient to lie on his/her back with the knee set at 90° flexion [16]. Then an anterior force is applied to the posterior tibia, with thumbs across the anterior side of the joint. The motion of the affected knee is compared to the unaffected knee and tactilely graded. The scale used in these tests are grade 1 through grade 3, with grade 1 being 5 mm displacement and grade 3 being greater than 30 mm [16]. The Lachman test is similar, except the knee is held at 15-20° flexion, and one hand holds the femur in place while the other pulls the tibia anteriorly. The examiner then tactilely grades the instability of the ACL, characterized by the endpoint [17, 18]. This is graded on the same scale as the Anterior Drawer test. However, these tests have been documented to have varying levels of reliability, with the Lachman test being reported as the most reliable [17,19,15]. A device that can objectively measure the laxity of the ACL is the KT-1000. B. E. Kilinc et al. used this device to quantify the accuracy of these tests and found the Lachman test to have 95% accuracy and Anterior Drawer test to have 61% accuracy [21].

The Posterior Drawer test is a method to help diagnose PCL injury [22]. In order to perform the Posterior Drawer test, the knee should be at 90° flexion and apply anterior to

posterior force on the tibia. Similar to the Anterior Drawer test, this is compared to the unaffected knee. The grades of the displacement relative to the unaffected knee are grade 1 up to 5 mm of motion, grade 2 up to 10 mm, and grade 3 over 10 mm. This method has been found to have 96% accuracy, and a sensitivity of 90% with trained surgeons [20–22].

In order to test the MCL and LCL, varus and valgus stress tests are conducted. To perform these tests, the knee is placed at 30°flexion then force s placed on the knee in abduction for valgus, and adduction for varus. Then a finger is used to tactilely feel the opening in the joint [4]. The American Medical Association grades the displacement in 3 levels: grade 1 up to 5 mm opening, grade 2 up to 10 mm, and grade 3 over 10 mm [23].

These clinical laxity tests help clinicians quickly diagnose injuries and compare knee laxity before and after surgery. However, research lab laxity tests like passive laxity envelopes can provide more comprehensive understanding of the knee's constraints and range of motion. Also, these lab tests can provide insights that cannot be practically obtained from clinical in vivo tests.

Reconstructive knee surgery can be performed if the damage is isolated, such as a tear or fracture that can be repaired. Often, when there is significant damage to the soft tissue and cartilage from arthritis, a total knee arthroplasty (TKA) or knee replacement surgery can be performed. TKA is a common procedure, with a 198% increase from 1994 to 2014 [25]. During the procedure, articular geometry is replaced by resecting the bone and replacing it with an implant. Depending on the component selection and the surgery, this gives varying levels of constraint based on the patient's needs. To give the patient the best possible outcome, ligament balance and the alignment of the knee need to be considered. When the ligaments are properly balanced there is equal ligament tension in both the medial and lateral sides of the of the knee. To achieve this, some surgeons will use kinetic sensors to more objectively balance the soft

tissue envelope [24, 25]. Gap balancing and measured resection are two TKA surgical

techniques commonly used to restore limb alignment and soft tissue balance about the knee [26,

27]. Gap balancing is a technique that resects the tibia to be parallel with the femoral

component, with both collaterals in tension [28]. The end result should be a rectangular gap in

the resected tibia to the femoral components and has shown to improve flexion stability [28, 29].

Griffin et al. studied 84 gap balanced TKAs and found that flexion gap differed from the

extension gap by no more than 3 mm [32]. This showed the consistency of the surgery and how

the results were repeatable. Measured resection is a technique that resects the bone based on the

bony anatomical landmarks, often the transepicondylar axis, without consideration of the soft

tissue. This is because the transepicondylar axis is the axis of rotation for the femur and is

defined by connecting the prominence of the lateral epicondyle to the medial epicondylar ridge.

Using this axis allows for better stability of the knee. One issue with using this axis is that it is

difficult to interpret the bony landmarks to make the proper resection [31–34].

Golladay et al. performed a study that had two groups, a surgeon-guided and an

instrument-guided group, to perform a TKA [35]. This study found that 50% of surgeon guided

cases were quantitatively balanced as measured by an instrumental tibial trial component, while

the sensor-guided group yielded 84% balanced cases [37]. In both groups, and in other studies,

the patients who had quantitatively balanced knees reported significantly better outcomes scores

[23, 26, 27, 35]. Having the soft tissue balanced can help maintain the alignment of the knee and

ensure the bones are properly aligned [38]. There are two axes that doctors use when aligning

the knee, the mechanical axis and the kinematic axis [28]. To align to the mechanical axis, the

hip ball, knee, and the ankle are aligned [39]. Alternatively to align to the kinematic axis, also

called anatomical alignment, a 3D alignment of the knee is used to replicate what is considered a

more natural orientation of the bone or to restore the normal 3D orientation of the 3 kinematic axes [26, 38]. Some studies have shown that a kinematic alignment has produced a more natural gait [41]. However, alignment based on the kinematic axis has a tendency to place more of a load on the medial side of the implant [27, 37]. This method has been shown to have increased malalignment and need more revision surgeries [27, 40].

Research Methods

TKA surgeries are predicted to increase in coming years, therefore, research on how to improve TKA implant designs and outcomes is ongoing [41–43]. In research lab knee testing, fresh frozen cadaver specimens are used to maintain the mechanical properties of the tissue [46]. Testing cadaver knee specimens can take many forms. Active and dynamic testing can simulate muscle activation and how the knee and soft tissues respond as it goes through dynamic motions, such as walking, squatting, or other maneuvers [45, 46]. Another type of active testing involves using knee machines to test wear patterns on implants [47]. These devices are useful for comparing the 6 degrees of freedom knee kinematics (Appendix A) of a native knee to its kinematics (or movement of the tibia with respect to the femur) after a TKA. These machines use a range of sensors in order to accurately measure the loads and kinematics of the knee [43, 46]. With the use of these rigs, researchers are able study how the knee will behave under active loading conditions. However to get a better understanding of how the passive structures behave without muscle activation, a knee envelope is performed [49]. Blankevoort et al. discusses that an envelope is needed to properly model the six degrees of motion about the knee [1]. Several styles of rigs and methods have been used to conduct envelopes [2]. Some involve robotic

mechanisms, some use manual manipulations of the knee, and some use static systems [9, 48–53].

Robotic rigs, using pneumatic cylinders, or static rigs which attach a known mass to the rig to apply a known force at flexion can be used [8, 51]. Both are similar in that the leg is set at a flexion angle and then a force is applied. The issue with these rigs is that they don't take into account the path dependency of the knee as discussed in Blankevroot et al. [1]. A way around that is to apply the loads as the knee is in motion through flexion extension. The method used in the EJBR Lab is the manual manipulation of the knee [51]. In order to record the data for manual manipulation, both the loading data and displacement must be recorded. Motion capture systems were used to collect the displacement at the joint. A commonly used motion capture system is an active marker system. Active marker systems use Infrared Emitting Diodes (IREDs) that are fixed onto a rigid body or machined frame holding the IREDs in place. The Optotrak system used in the EJBR Lab is an active marker system that has a resolution suitable for recording the displacement about the knee [54]. The system has a documented translational error of 0.2%-2.0% and a rotational error of 0.8-2.0% [55]. This system is not without limitations. The IREDs need to be a distance of 1.75 meters away from the camera to help keep the noise of the system to be 0.04 degrees or 0.03 mm or below [56]. The applied isoload is recorded with a triaxial loadcell, which is a set of force transducers that can record forces that act on it and in what direction they are acting.

The probe point data collected are used to create the coordinate system for the passive laxity envelope. Grood and Suntay were able to accurately measure the six degrees of freedom in the knee utilizing the axes of rotation and anatomical landmarks [57]. Just like using the

boney structures in surgery, there is some uncertainty involved with collecting these probed points [58].

Manual manipulation of the knee does not allow for the exact dictation of position and load, therefore, the desired position and load must be extrapolated. The radial basis function (RBF) weighs the points relative to the values around it allowing for a smaller bias to outliers [59, 60]. A flow chart describing how the RBF calculations work as described by Cyr et al. can be found in Fig. 3 [58]. Using the RBF to generate a prediction of the knee envelope creates a 3D isosurface of the displacement at a given load. The highest errors in the RBF occur where there are large gaps in the data. Boppart et al. looked at using sequential down sampling to give a confidence in the collected envelope [60]. This process involved using every fifth point in the data set to generate one path, and then followed up with another set of every fifth point in the data set. This was repeated with every 10th point, 15th point, and 20th point, generating several paths. By creating multiple predicted paths of the same envelope, confidence in the prediction can be observed. Boppart et al. also used this sequential down sampling method to look at how different investigators affect the outcome of the same knee [60]. This sequential down sampling process can also be used to compare the variation in predictions across multiple knees. When conducting multiple knee envelopes, it is common practice to have a standard protocol to help with consistency. Sequential down sampling allows comparison of points of higher variation, and if changes can be made in order to achieve better results.
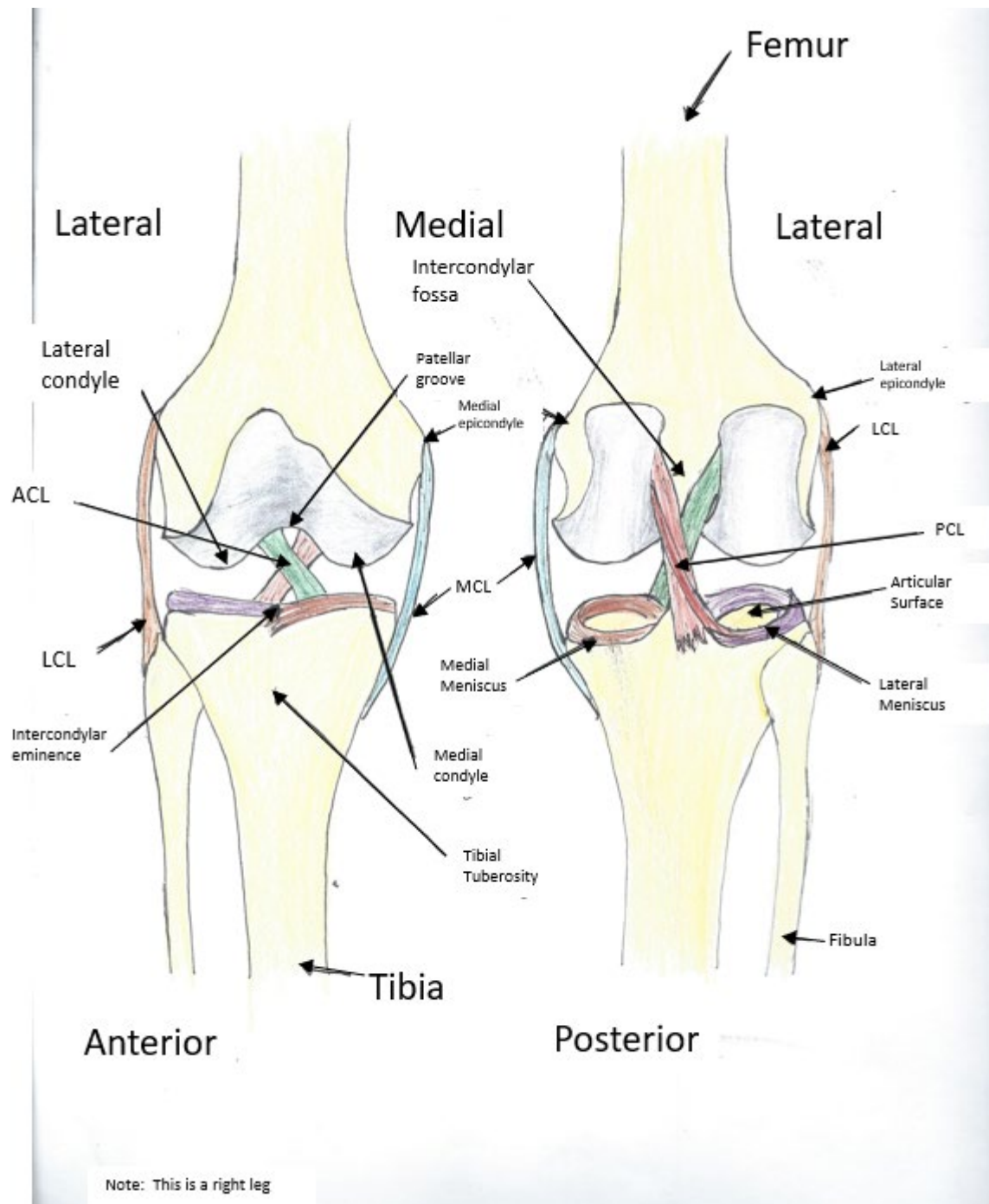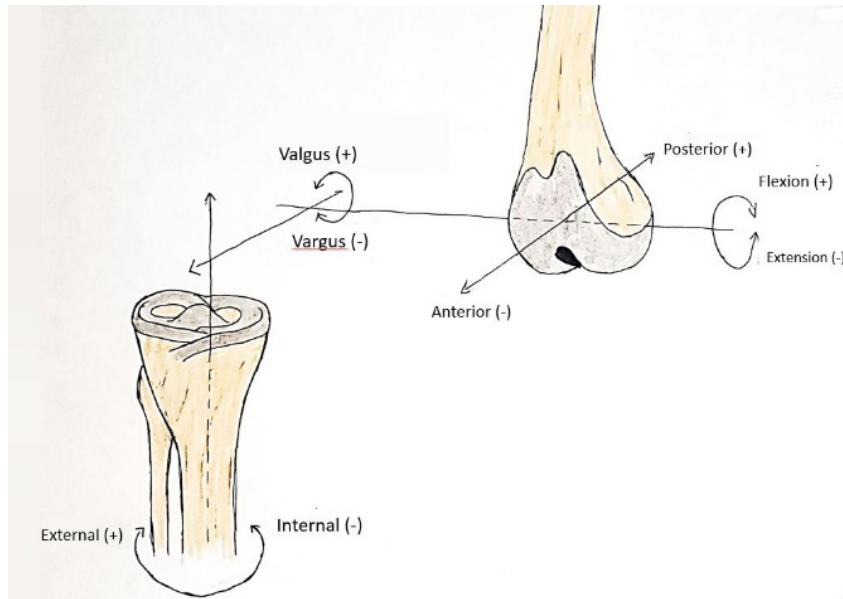
Fig. 1: An anatomical representation of the knee.

Fig. 2: A representation of 6 degrees of freedom. Superior/Inferior and Medial/Lateral translations are not labeled but axes are present.
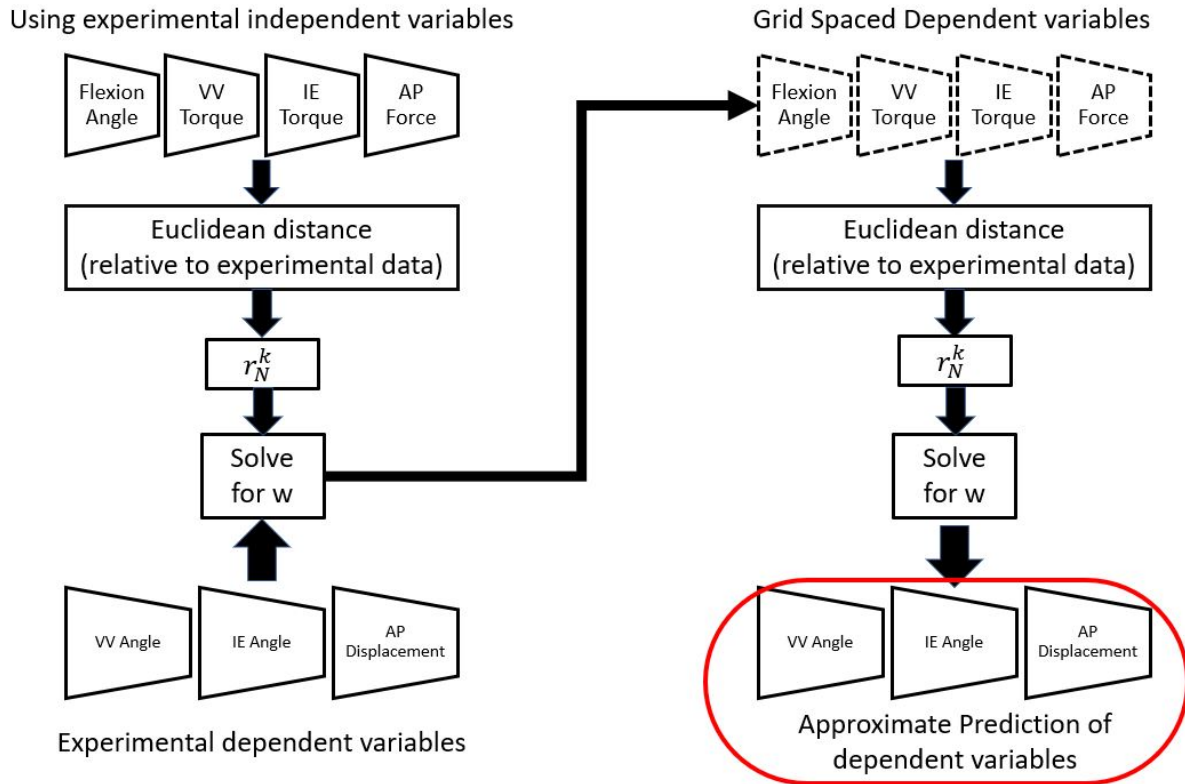
Fig. 3: Flow chart of the RBF generating the prediction in the envelope [59].

Chapter 3: Measuring and Improving the Quality of Envelopes of Passive Constraints

Introduction

    The motion of the knee is dictated by the applied loads and anatomical constraints, such as the articular surfaces between the tibia and femur. A common kinematic analysis performed to understand the role of those constraints is a knee envelope [1]. Passive envelopes, or envelopes observed without muscle activation, measure the relative motion of a joint under certain loading to understand the constraints from the articular surfaces, the ligaments (ACL, PCL, MCL, and LCL), and other soft tissue structures, without requiring active motion from the subject. These envelopes give an understanding of knee motion without muscle activation as

described by Blankevoort et al. [1, 48]. Traditionally the knee envelope is performed by putting the knee in a VV, IE, AP, or combination of these positions, then moving it through flexion extension, giving a two-dimensional understanding of the constraints. The EJBRL created the unified envelope that allows the investigator to manipulate the knee through a series of motions to gain an understanding of the constraints and give the investigator more freedom of motion when preforming the envelope procedure. Clinically, passive laxity tests are used to determine if any structures in the knee are damaged [20]. Surgeons use knee envelope studies, along with evaluations of a knee's balance and alignment to improve patient knee outcomes.

During a TKA operation, surgeons manipulate the knee by hand and use trial components to evaluate the balance of the knee and the alignment of the implant [61]. If the knee is unbalanced, the ligaments can be partially resected or released to improve balance [62]. The most broadly accepted definition of a balanced knee discussed in literature includes the following components. The knee must have a full range of motion. There should be a symmetrical medial-lateral gap at full extension and at 90 degrees flexion, the gap must not have medial-lateral tightness or laxity. The patella must be well-tracked and it must have correct rotational balance between the tibial and femoral components [63]. Improvements in assessing the balance of the knee during these procedures might improve the outcome of the surgeries, the life of the implant, and the quality of life for the patient [43]. Over time, imbalances in the knee can cause misalignment and aseptic loosening which is a leading cause for prosthetic failure with total knee arthroplasty [64]. A TKA procedure strives to achieve not only the balance of the knee, but also the correct thickness of the tibial insert and proper knee alignment. Both balance and good alignment must be achieved to improve the performance of the knee and longevity of the TKA procedure. Having misalignment or imbalances in the knee can lead to more sliding

motions and greater pain in the knee [63]. Proper knee alignment occurs when the knee has equal varus and valgus motion relative to the mechanical or kinematic axis. Mechanical alignment, or aligning the hip ball through the knee to the ankle, is the more traditional method and is widely used in practice [40]. Kinematic alignment is a newer technique that gives a more natural motion to the patient while walking or performing other tasks [40]. Proper alignment contributes to a better-balanced knee and an overall better outcome with the implant [66, 67].

In addition to balance and alignment, there are several other factors that influence the surgeon's decision on how much constraint a patient needs for their knee. There are a range of techniques to help understand how constraints behave under different conditions. Utilizing these techniques investigators can further understand how a TKA operation changes the knee kinematics. One technique used is to apply a weight and maintain a VV torque on the tibia while the femur is fixed, then manipulate the knee through flexion extension to record the kinematics [2, 6]. Another technique is to use a robotic manipulation of the knee that holds the knee at specific flexion angles and displacements and then measures the amount of force required for that movement [2, 29, 48, 51, 68–70]. These envelopes give a lot of good information for one dependent variable and generate a 2-D graph. These laboratory methods use fresh frozen cadaveric specimens allowing for experimentation without hurting a subject. The use of fresh frozen specimens helps retain the mechanical properties of the ligaments, as opposed to embalmed specimens or specimens that have been preserved through other means [70]. Cadaveric specimens also allow the observation of how knee modifications change the kinematics of the knee, such as doing multiple trials with different knee implants. Data gained from these analyses help engineers improve implant designs for greater stability, performance, comfort, and longevity [71].

The radial basis function (RBF) which creates the prediction of the unified envelope of passive constraint, is based on the weighted interpolation of positions relative to given loads collected from cadaveric specimens [73]. The unified envelope of constraint was created by the Experimental Joint Biomechanics Research Lab at the University of Kansas. It is a prediction of the envelope of the knee's function which uses an RBF to provide an approximation of the relationship between applied forces and the observed kinematics and predicts the composite of constraints provided by that knee's structures, articular surfaces, ligaments, and soft tissue, for a given degree of freedom. By utilizing the RBF multiple variables can be observed and compared and generate a 3D representation of the information, giving a better representation of how the variables influence each other. The RBF gives investigators the ability to use manual manipulation rather than needing a fixture to move the specimen to specific locations or applying specific loads.

Boppart et al. [60] used a sequential down-sampling process (SDSP) to create multiple subsets of data from the same knee trial in an effort to understand the dependency of the prediction on segments of the data set. The method used a number of different subsets of data, and each subset was then used to generate an envelope prediction. By comparing the different predictions for any given position, the SDSP technique can provide a clearer prediction regarding the quality or confidence of the prediction. Boppart's work added clarity to understanding a knee envelope prediction from previously collected data. This study aims to build on Boppart's study and the SDSP technique to help improve data collection for passive knee envelopes at the time of collection, rather than just in an after the fact analysis. It continues to develop this useful tool by building on the previous SDSP work to identify areas of highest variation in the

predictions, developing an envelope quality scoring method for evaluating existing data sets, and creating a live feedback system to improve data collection for future studies.

The objectives of this study were:

1. Building on the previous SDSP work, identify areas of highest variation in the predictions based on the data collected from multiple knees, and seek to understand if there is a consistent reason for the variations.

2. Use the findings from objective 1 to develop an envelope quality score that investigators can use to evaluate how an existing data set will generate a quality envelope prediction for a given isoload.

3. Create a live feedback system which helps the investigator collect appropriate data for the desired prediction. By producing a live feedback of the envelope development that displays where additional load data needs to be taken during the current trial, it guides researchers to collect data more efficiently and effectively to provide the RBF with a high enough quantity and distribution of experimental data to generate higher quality envelope.

Methods

The experimentation starts within 24 hours of thawing a fresh frozen cadaver specimen. The knee is then dissected by removing the flesh from the specimen 5 inches to 10 inches away from the flexion axis of rotation on the bone end. The bone is then cut at 7.5 inches from the flexion axis of rotation. The cut bone ends are centered in aluminum pots and secured into place with PMMA cement. The femur is secured onto a structure to prevent the femur from moving. A 6 DOF triaxial load cell (JR3 Inc., USA) is attached to the distal end of the tibia. Optotrak

rigid bodies with 6 IREDs on them are placed on the proximal end of the femur and on the distal

tibial bone end, with an additional rigid body used to probe different points on the system (Fig.

4). The Optotrak Certus system is used to record the motion of the rigid bodies and record probe

points. During experimentation, the knee undergoes a passive flexion extension motion to

measure baseline kinematics of the knee. The knee then undergoes the following combination of

loads: a VV motion (back and forth in the varus valgus directions while the knee runs through

flexion extension); IE motion (through internal and external motion while going through flexion

extension); VV with IE (put through a varus motion followed by and internal and external

motion, then a valgus motion followed by internal external motion throughout flexion

extension); the final motion is IE with VV, where the investigator puts internal motion on the

knee followed by both varus and valgus motions, then an external motion followed by medial

lateral motion. Probe points are taken on the knee as shown in Appendix B. During this part of

experimentation, the investigator uses the feedback screen to make sure they are applying

enough force and collecting data across the entire envelope.

Once the data are collected, they are processed in a MATLAB (The Mathworks Inc.,

USA) program, using the radial basis function (RBF). The RBF is an interpolation tool that is

used to create an approximation of the knee envelope from the collected data. Since unified knee

envelopes use several dimensions of information, the RBF is able to better approximate the knee

envelope than other methods such as polynomial and spline predictions. A 3-D prediction is

generated from the study. Two mesh graphics are generated from the data sets: the isoload

surface and the kinematic envelope. The first surface is the isoload surface which generates a

cylindrical mesh. The second surface uses the same type of mesh but uses the kinematic

predicted dimensions rather than the torque dimensions. To better understand the variations in

the prediction, the data are run through a sequential down sampling process (SDSP) [61]. This is a method of taking a single set of data and creating multiple subsets of data from it by taking every 5th, 10th, 15th, and 20th experimental data points in the data set and creating additional interpolation predictions from each of them. This results in the investigator having now 50 new sets of data that can be run through the RBF and the resulting predictions can then be compared to understand how much variation there is in these predictions. If there are few areas of high variation, one can place greater confidence in the prediction.

The analysis performed for objective 1 used data sets from 13 cadaver knees that were tested within 24 hours of thawing (9 right and 4 left, average age 59 (SD 10.15) years, average BMI 24 (SD 3.35)). All 13 data sets were collected using the same protocol which consisted of passive manipulation through the knee's flexion extension range of motion using internal/external torque, varus/valgus torque, and anterior/posterior force. The average and standard deviation of the variations for the 13 data sets as a group was taken and mapped onto the average envelope shape to understand and compare the locations of the areas of higher variation and if the magnitude of those variations is consistent between different knees. An example of an envelope surface mesh with the variation being overlayed onto this mesh is shown in Fig. 4. The same figure shows the vertices that are produced by the grid of the generated mesh. All envelope predictions are at 8000 Nmm and the graphs are color coded with red showing areas of high variation and blue showing areas of low variation. This visual display of areas of high variation shows the differences in locations of high variation for individual knee envelopes. In order to understand local variation for each of the 13 knees, the variation in the IE direction was scaled to be 0 to 1 then was averaged together with the VV variation that was scaled in the same manner. The variation is scaled to understand the location of higher variation

18

for each knee and is not used to compare variation values. All investigators followed the same instructions for the data collection for the 13 knees. If the areas of highest variation are consistent among the different knees, it might indicate a possible source of variation due to the protocol.

Objective 2 was to create an envelope quality score that can be used in evaluating existing data sets for generating useful knee envelopes. Because the radial basis function weights experimental points that are closer to the interpolated position more heavily than points that are farther away, an existing data set can be analyzed based on the distance, quantity, and distribution of the experimental data points relative to a given isoload to generate an envelope quality score. This calculation was titled the "envelope quality score" because a higher score indicates the passive knee envelope generated from that data set has a sufficient quantity of data relative to the isoload to generate a knee envelope. To generate a quality score, the quantity of experimental data points is totaled if they are located within a Euclidean norm distance of 0.25 away from each vertex in the envelope isoload surface as shown in Fig. 5. The envelope quality score for each of the 13 knee data sets was generated and compared to understand how the current protocol is impacted at different isoloads. A higher envelope quality score indicates the suitability of an existing data set for producing a viable passive envelope prediction at given isoloads. Having data collected around the desired isoload means the RBF will have less variability and therefore more confidence in the prediction. Thus, calculating a quick envelope quality score will help researchers quickly evaluate existing data sets before they conduct extensive analysis on the data only to find that it will not provide a desired envelope prediction. Although this study did not try to determine what an ideal envelope quality score would be, generally a higher value should produce an envelope with less variation.

Objective 3 of this study was to create a new feedback system which enhances the initial collection of data. The current feedback system (Fig. 6) shows what load has been applied and visually displays the current load with a contrasting white box. This white box shows where the load is being currently recorded and as more data are being collected the color of the boxes changes from red (indicating little amount of data) to blue (getting more data). The proposed new feedback system developed in this study replaces the current feedback screen and displays an isoload surface showing where the experimental data being collected are relative to the isoload, and a prediction feed of the RBF envelope to give the investigator an idea of the envelope they are targeting and when the investigator has collected enough data that the prediction does not change. Because the feedback needs to make this prediction in real time, the program (Appendix C) removes information that does not have as much weight to the related envelope. Therefore, the only points that are used in the feedback screen are points that are within 500 Nmm of the isoload. This feedback system requires the investigator to input the desired isoload before the experimentation and manipulation begins, to help the investigator focus on collecting data around their desired isoload. This system could be rerun with different isoloads to understand how well the data generates a variety of different isoloads. This was tested with three manipulation methods; the traditional method (the method the 13 knees underwent), the wall method, and the spiral method. The wall method involves holding the knee in a position near the desired isoload and then running through flexion extension. The spiral method involves applying a shifting load on the knee making a circular motion as the knee goes through flexion extension, while maintaining loads close to the targeted isoload. These three manipulation methods were evaluated to determine if the methods of manipulation made a difference in the data collection outcome.

Results

Objective 1 was to analyze previously collected envelope data from 13 knees and identify the areas of high variation for a desired isoload to determine if the areas of high variation were consistent. A consistent location of variation might imply that the variation may be due to the way the experiments were run or instructions given the investigator. This analysis showed that the areas of high variation were not consistent in their location (Fig. 7A). This was further confirmed by analysis of the average variation (Fig. 7B) and the standard deviation (Fig. 7C) across the knees on an average envelope. Showing no consistent variation for these measures across the entire envelope, these data demonstrated that the variation does not occur in consistent areas and therefore was not likely due to instructions given to the investigator.

Objective 2 was to create an envelope quality score so investigators can evaluate how well an existing data set will fit an isoload to make a generated envelope prediction. Fig. 8 shows the quality score for a specific data set over several different isoloads. For this knee it has a higher quantity of data at the lower isoloads, and less data for the interpolation of the data at higher isoload values. Fig. 9 shows the quality score for the 13 knees at isoloads ranging from 0 to 20,000 Nmm that were collected using the same protocol. The graph shows how the protocol collects more data at the lower isoload forces, showing the prediction follows the data at those lower forces. Fig. 10 displays how the different methods of manipulation affect the fit of the prediction relative to the data, with a better fit when data are collected in a way that is distributed more closely to the target isoload. A typical example of how the variation changes across isoloads is shown in Fig. 11 which shows predictions based on four different isoloads (2,000 Nmm, 10,000 Nmm, 15,000 Nmm, and 20,000 Nmm). The left most graph shows that for a low isoload of 2,000 Nmm many of the data points collected, shown in red, fall inside the target

isoload and therefore exhibit low variation from the predicted envelope. The right most graph shows that for a high isoload of 20,000 Nmm the data points fall a greater distance from the target isoload surface and therefore exhibit high variation from the predicted envelopes. In this example, we see that more experimental data points were collected around the low isoload of 2,000 Nmm and fewer experimental data points at higher forces like isoloads of 15,000 and 20,000 Nmm.

For objective 3, the proposed new feedback system developed in this study would replace the current feedback screen and display an isoload surface showing where the experimental data is being collected relative to the target isoload on the left, and a prediction feed that shows the developing RBF envelope prediction on the right (Fig. 12). Fig. 13 shows how the new feedback screen will help guide the investigator by showing on the left how close the collected data points match the target isoload, highlighting in red where more points need to be collected. On the right side of the feedback screen the evolving envelope prediction is displayed. Again, as the investigator collects the appropriate data, the surface will turn from red to blue. Fig. 14 shows another example of the development of data collection relative to the isoload as it would be displayed on the left side of the feedback screen and how adding the proper data points results in the surface evolving from mostly red to mostly blue. Fig. 15 shows the right side of the feedback screen taken at six points during the collection process and how the envelope prediction similarly evolves as the data are collected. The program is able to update in one second increments, as shown in Fig. 16.

Discussion

Objective 1 of the study was to review the envelopes generated from experimental data from 13 knees, all collected using a similar protocol. The statistical down-sampling process was used to study similarities in the location of the areas of higher variation in the envelope. These variations were then normalized across IE and VV directions at an 8000 Nmm isoload for the knees to examine if areas of higher variation might share some pattern that indicates the source of variation. By examining the variations across multiple knees (Fig. 9 and Fig. 7A) the average variation (Fig. 7B,) and the standard deviation (Fig. 7C,) no common trend in the location of the variation was apparent, suggesting that the protocol was not inherently causing high variation in consistent knee positions. However, the RBF process weighs data points that are closer to the desired interpolated position more heavily than those farther away, so the quantity and distribution of data points collected should be guided by the desired isoload to produce a better envelope. By prioritizing points close to the desired isoload surface, the prediction can be made with less variation and more confidence at interpolating the experimental data. This suggests that the testing protocol is not creating consistent irregularities in the data collection, instead other factors are the cause of variation in the prediction.

Objective 2 of this study focused on the envelope prediction quality score, calculated based on the quantity and distribution of data relative to a given isoload. Since the RBF is an interpolation process, which weighs the data based on how close they are to the desired isoload, collecting data points distributed more closely to the desired isoload should produce a more confident prediction with less variation in the prediction. The results of the envelope prediction quality scoring demonstrate how the previous protocol led to the under collection of data points

at some desired isoloads. By applying this quality score analysis to existing data sets, investigators can use this envelope quality score analysis to focus on data sets which contain the quantity and distribution of data most likely to generate a knee envelope at a target isoload with a lower amount of variation in the prediction.

Usually, it is more valuable to study the higher loads where the ligaments have a greater influence on the knee's motion.   Previous studies have shown that a torque of 8,000 Nmm is needed to show the elastic linear region of the ligament [21], [72]. Although the lower loads do hold valuable information, the linear elastic region generally is the region most studied by researchers. If data collection focuses too much at lower isoloads, at the expense of higher loads, there will be fewer points within the range of the envelope at higher loads and result in a lower quality score and less confident envelope prediction. The previous protocol used on these knees produced envelopes with more data at lower loads, rather than the targeted isoload, with the confidence in the higher isoload envelopes eventually getting so low that the prediction was not valid. This can be seen in Fig. 11 where the 15,000 Nmm and 20,000 Nmm envelopes show greater variation in the prediction as well as fewer points within the range of the envelope. Therefore, being able to generate a quality score based on the quantity and distribution of data around the desired isoload gives the investigator an efficient way to evaluate an existing data set to determine if enough data at a specific isoforce has been collected to make a confident prediction. A data set with a higher quality score will yield a prediction with less variation. This insight can also be used to guide investigators to avoid spending excessive time collecting additional data that may be unnecessary for their research goals.

The most efficient and effective procedure is to gather data for the envelope that falls close to the desired isoload. By determining how well distributed the data is for a specific

24

isoload, a prediction can quickly be generated to tell the investigator in real time what envelopes are viable based on the quantity and distribution of the data collected for their prediction.

Objective 3 of this study was to develop and present a new feedback system for investigators which shows the collection of data around the target isoload and development of the knee envelope in real time. This allows the investigator to visually see when sufficient data has been collected to fill out the envelope and to see where in the envelope more data are needed around the desired isoload. The value of this new feedback screen is not simply that it allows the researcher to quickly identify where they should collect more data for an improved envelope,it also provides near live feedback to the researcher, allowing them to more effectively and efficiently collect data during the initial test while the cadaveric specimen still maintains its soft tissue and mechanical properties. Therefore objective 3 of this study was to develop a MATLAB program that tells the investigator in real time how they need to manipulate the knee to generate data around the desired isoload for more efficient data collection. This progressive feedback screen gives the researcher information about their distribution and quantity of data as they are collecting it, not only helping researchers ensure they collect the proper quantity and distribution of data points, but also guiding them in collecting data points to produce the desired envelope more efficiently.

Fig. 13B shows the same trial data used in Fig. 13A and C except in this example, the prediction collected only pure VV data initially, resulting in a slower and less complete processing of the prediction calculation. Since the prediction in Fig. 13B is not filled out, only having points on the VV axis, the prediction is incomplete. If the investigator collects the data along the valgus edge of the isoload, using combinations of loads around their desired isoload, instead of going back and forth between varus and valgus, they will develop the envelope more

quickly and more efficiently. This is because the new feedback screen guides them as they go to collect those data points most critical for the developing envelope. These data most similar to the targeted isoload surfaces are used to make a quick simplified prediction. This can also be seen in Fig. 10 and Fig. 17, which show the quality score of the same knee using different manipulation methods. The highest quality scores come from focusing on collecting data near the desired isoload. Both the spiral and wall methods of manipulation allow the investigator to get to a higher quality score more quickly and efficiently than the traditional method, shown in Fig. 17. The RBF prediction generates a visual mesh illustrating the prediction of the envelope. A lower density mesh produces a faster prediction, but with less clarity. While efficiency of data collection is certainly not as important as the effectiveness of data collection, it is a nice practice in general to work both effectively and efficiently. This would improve not only the efficiency of the testing process, but the quality and usefulness of the envelopes produced.

There are some limitations to the work presented. In general, all data collected for passive envelope studies is assumed to be accurate for the target isoload of that study. This can be a limitation in that investigator application of target loads through differing manipulations can result in different ending positions at that load and increase areas of variation in predictions.

For objective 1, some inaccuracies could have resulted from various factors such as slightly different manipulation motions as data were collected, differences in knee kinematics, differences due to knee demographics, etc. However, since the focus of the study was how the data was collected vs. the resulting envelope, these possible sources of inaccuracies should not invalidate the results of this study. For objective 2, the envelope quality score was not tested to find an ideal quality score for a particular study or question. Rather, it was designed to measure

how a given data set contained the quantity and distribution of data relative to a given isoload needed to produce a confident envelope prediction. While the quality score analysis can help investigators determine which existing data sets are most likely to generate a viable envelope for a desired isoload, it does not to tell investigators the ideal quality score value for a particular study. Based on their study objectives, the investigator must still determine the most appropriate isoload for the knee envelope. Another limit in the quality score is that it does not have a limit and the increase in quality is nonlinear. As the investigator continues to add data around the target isoload, there is a point of diminishing return. It is up to the investigator to determine when a high enough score is sufficient.

For objective 3 the envelope quality score is not calculated and displayed in real time. The proposed feedback screen shows the envelope developing in real time as the data is collected, and this should minimize areas of high variability in the resulting envelopes. However, if the envelope quality score could also be displayed as data is being collected, it might add even greater confidence in the initial data collection process. The calculation of the envelope quality score currently requires the whole set of data to be fed into the calculation. In future studies, if the envelope quality score could be calculated as the data is being collected, it could lead to an even more efficient and confident data collection process. Another future improvement that might be made is to show the quality score over the surface of the envelope prediction to give the investigator more of an understanding of the quantity and distribution of the data in local areas rather than as a whole. Finally, the new feedback system requires the desired isoload to be identified, but future development of the feedback screen could allow the investigator to change what isoload to focus on or, if the investigator wants to collect additional data that could be useful in future studies with a different area of focus.

27

This study builds off of previous research done in the Experimental Joint Biomechanics Research Laboratory and gives a direction for how knee envelope research can be conducted in the future. Future studies can look to improve the efficiency in the program to reduce the computational requirements resulting in a feedback that computes all the information more quickly and increases the potential to be useful in clinical settings. It also is a steppingstone in getting these tools in the hands of medical professionals and further helping patients.
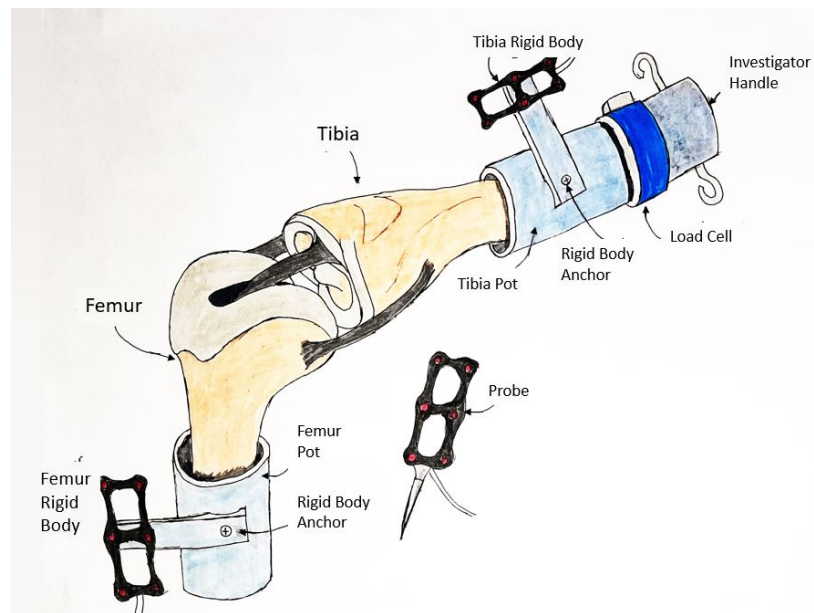
Fig. 4: The experimental set up of cadaveric knee with motion capture attached with a fixture on the two bone ends. The triaxial loadcell is placed on the tibia, as a handle for manipulation.
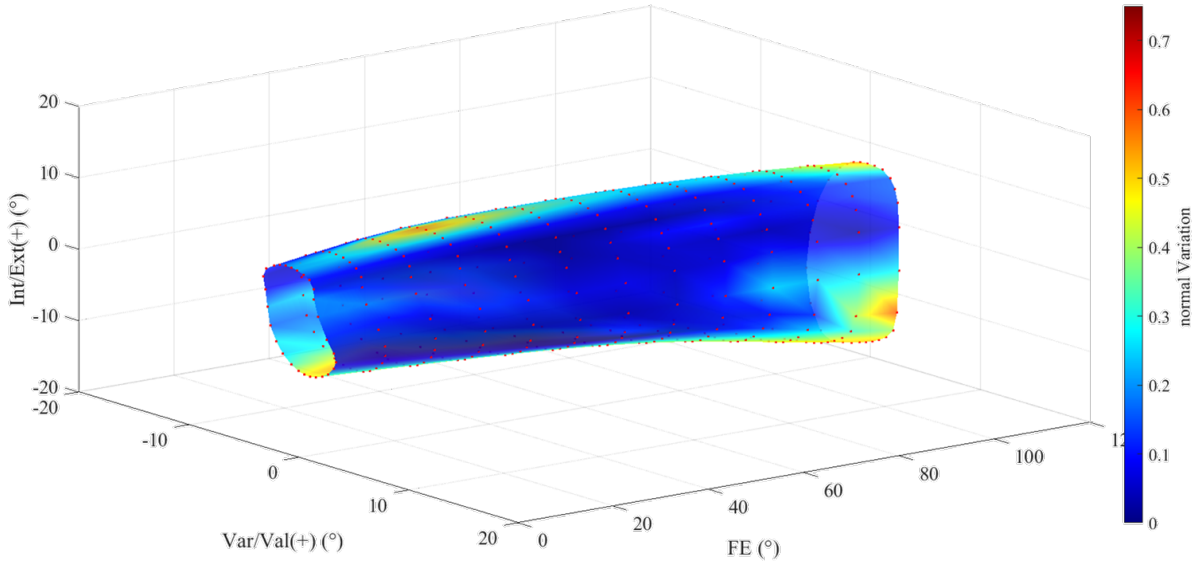
Fig 5: The unified envelope displaying the 3d mesh grid at 8000 Nmm of force. The vertices in this grid are used in finding the density and distribution of data and can be found as the red dots on the surface. The SDSP variation is overlayed on the mesh to give an understanding of the locations of higher variation.
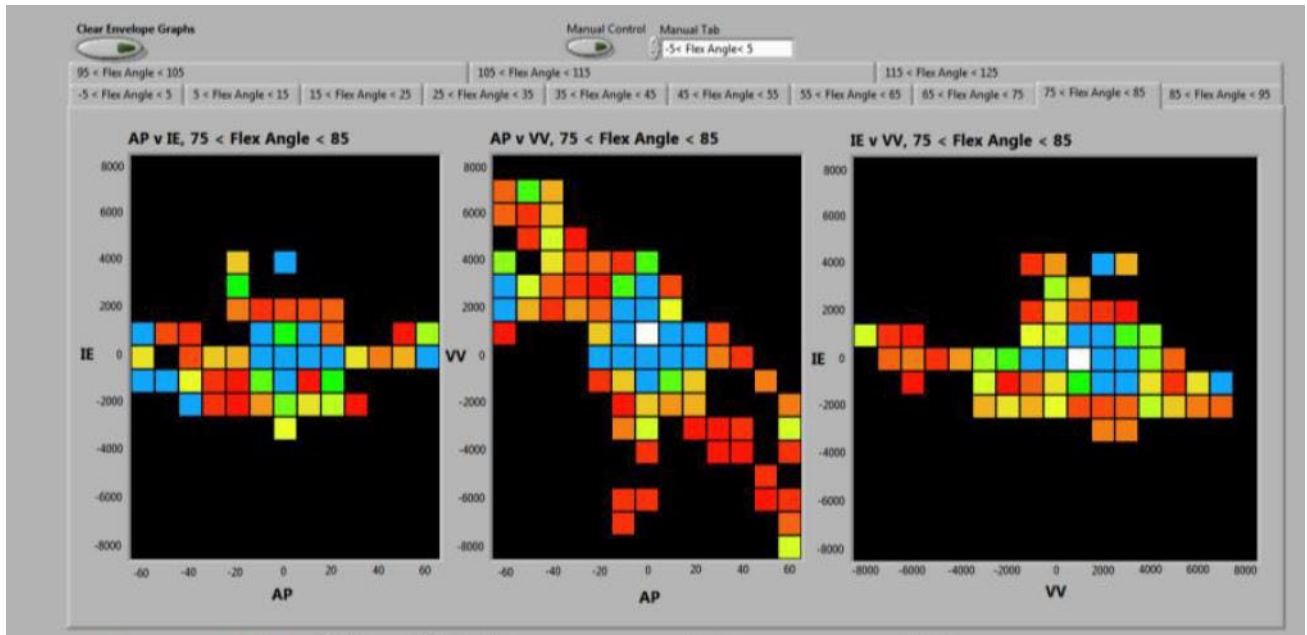
Fig. 6: The existing feedback panel, each graph represents the different combinations of loads. This white square represents the current load and the different colors show how much data are present at that combination of force, going from red to blue as more data get collected.
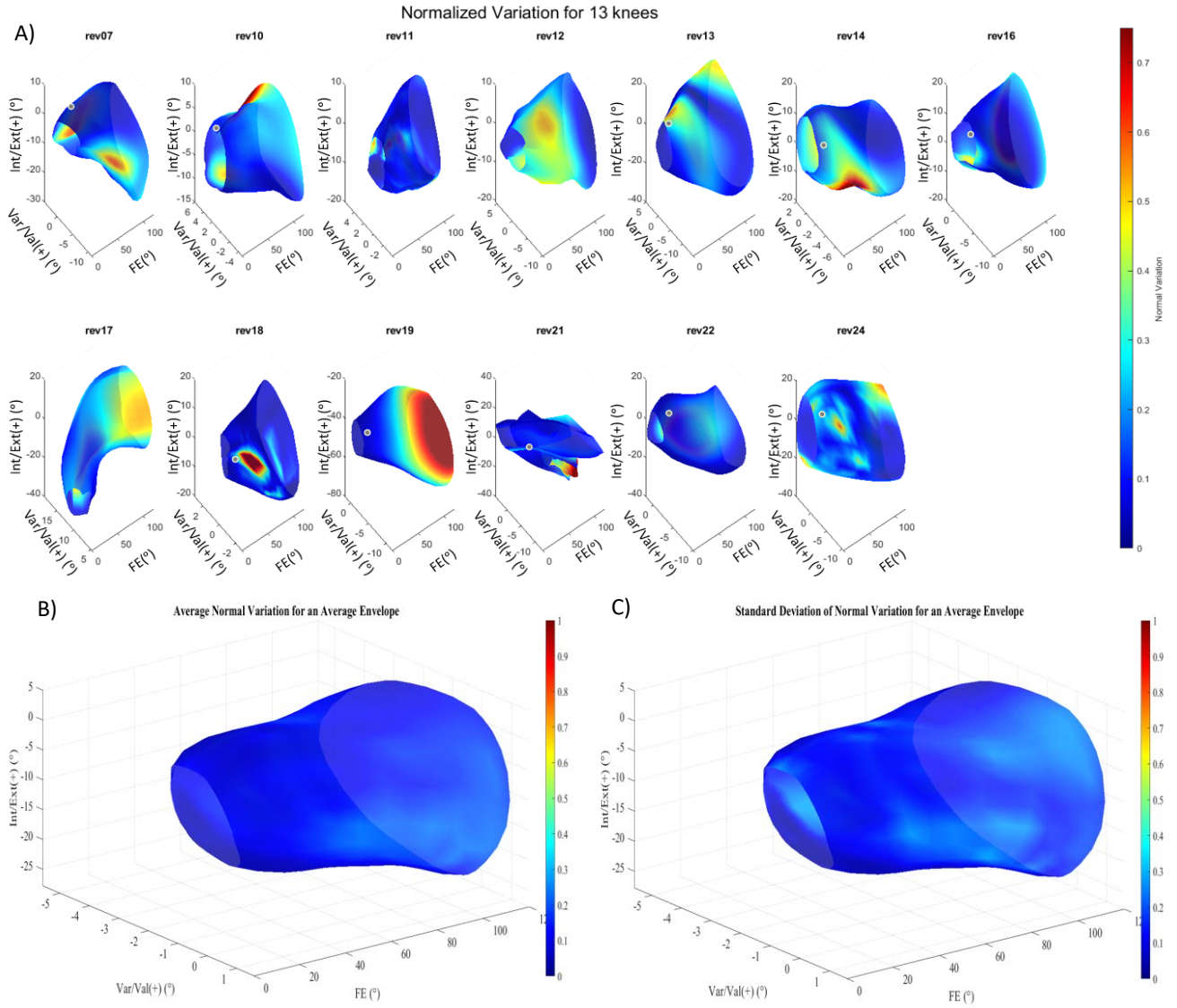
Fig. 7: A)Plots for each of the 13 knees tested using the traditional method. The color is showing the points of higher variation for each knee, with red being high variation and blue is low variation, all envelope predictions are 8000Nmm. B) The average envelope showing the Average Variation across the 13 knees. B) The average envelope showing the Standard Deviation across the 13 knees
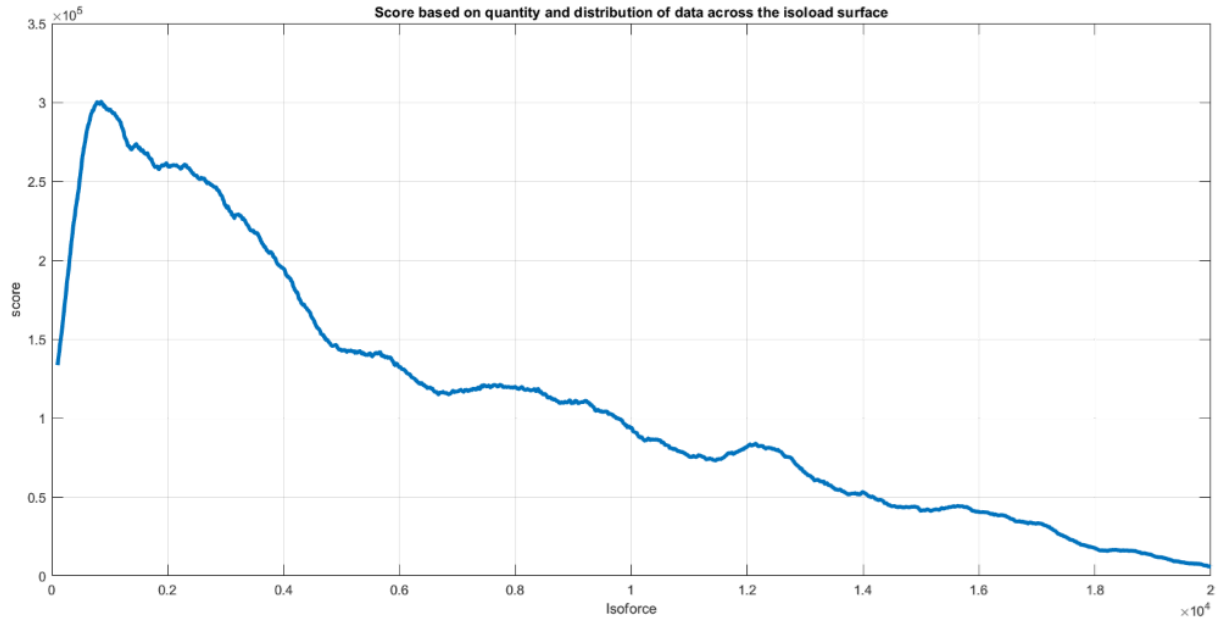
Fig. 8: The quality score plot of a knee showing how well the data quantity is distributed across multiple isoforces. This score would suggest that the envelope predictions would have less variations at lower isoloads.
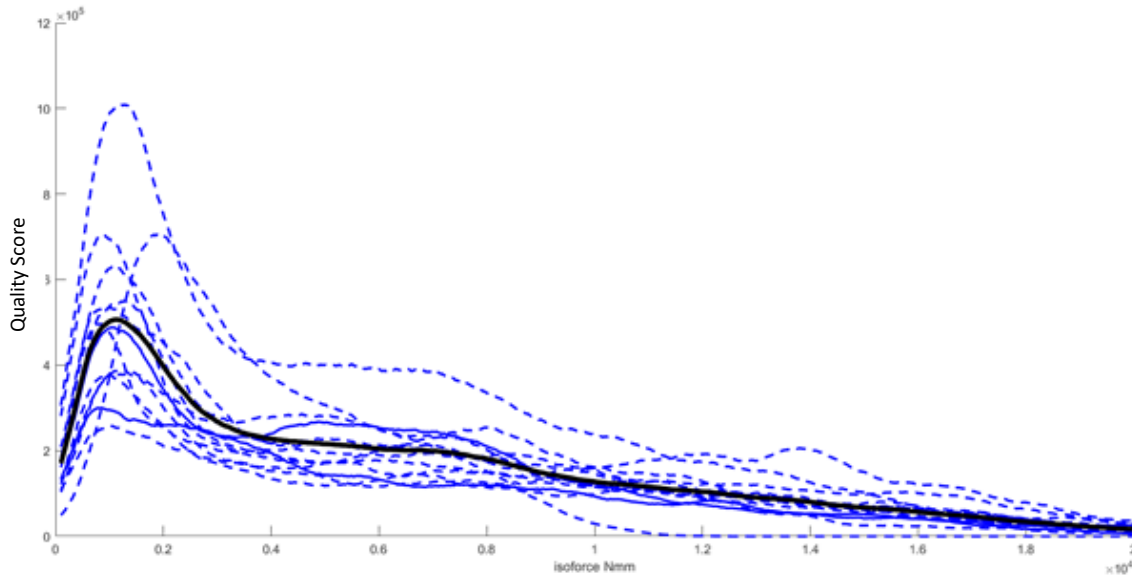
Fig. 9: This graph is showing how well the data quantity and distribution fit across multiple isoforces for all 13 knees, represented by the blue dashed lines. The average line is the black, showing the average trend of the score.
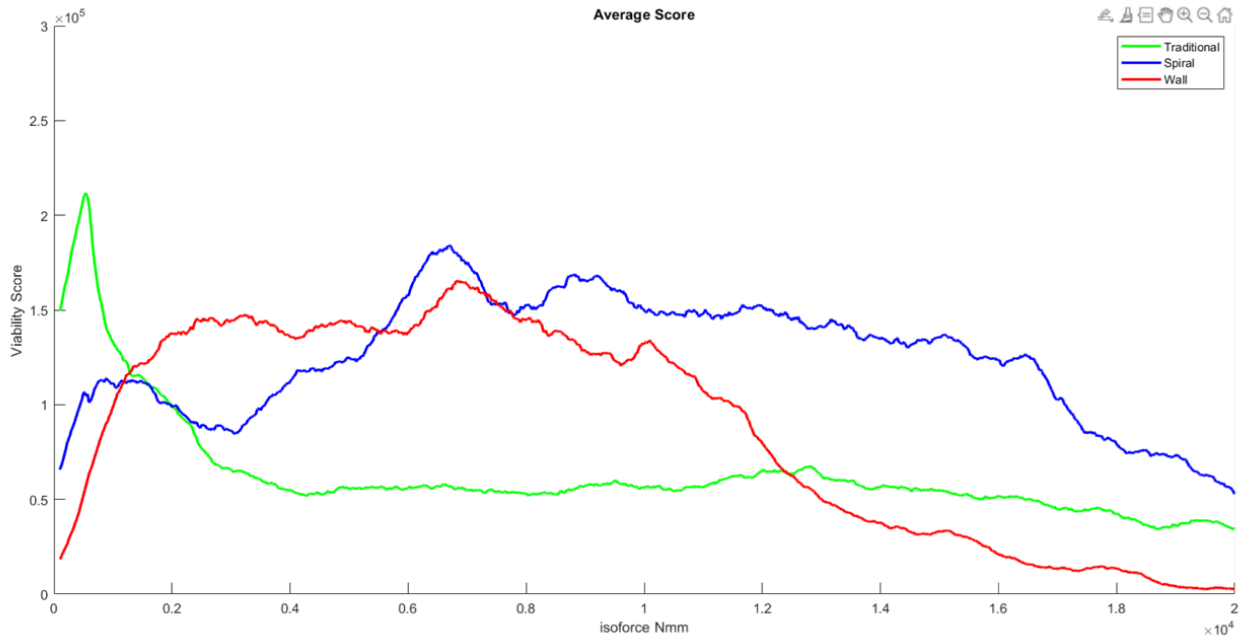
Fig. 10: Quality score using different methods of manipulations, Traditional method (in green), spiral method (in blue) and the wall method (in red).
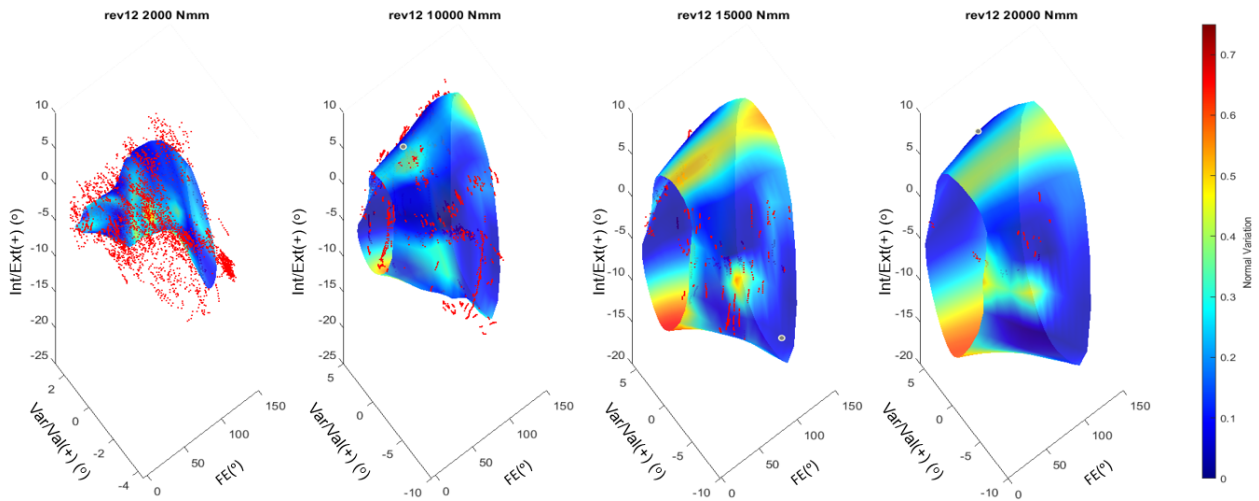
Fig. 11: Representative knee predictions at different isoload predictions. The left graph is a low isoload prediction and the graph on the right is a high isoload prediction. The color is showing the points of higher variation, red is high variation and blue is low variation. The red points are the experimental data that falls in the range of the isoload.
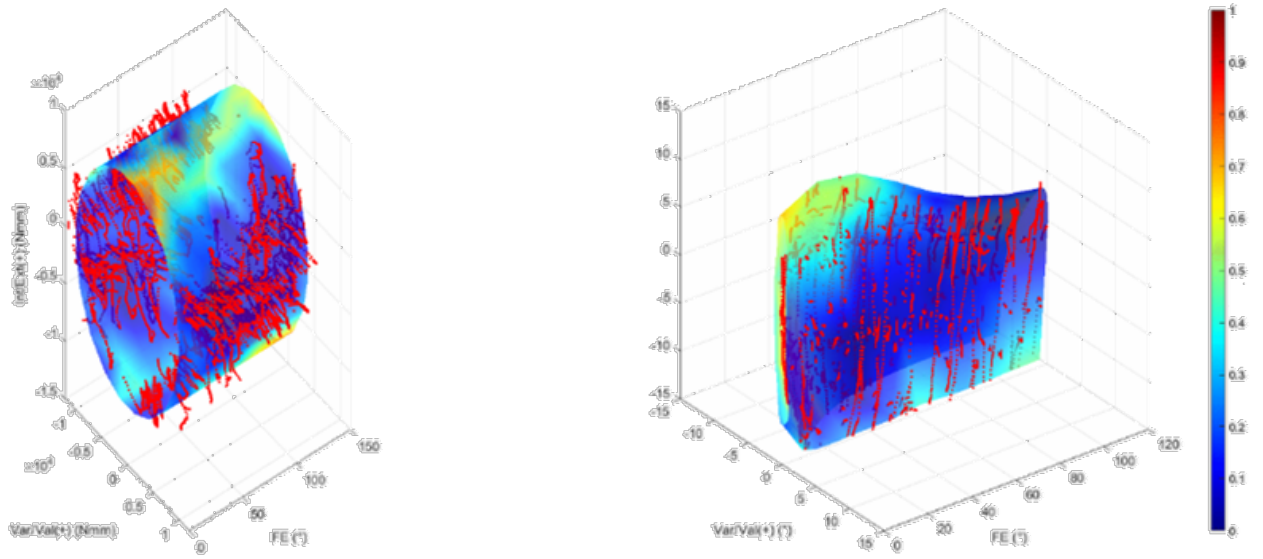
Fig. 12: The proposed feedback system showing the Isoload as a surface of the left and the development of the prediction as the surface on the right. The red points are showing what experimental points are collected that fall within the range of the desired isoload. The color of the surface is a representation of the data close to the desired location, with blue showing points are close and red being points are far away.
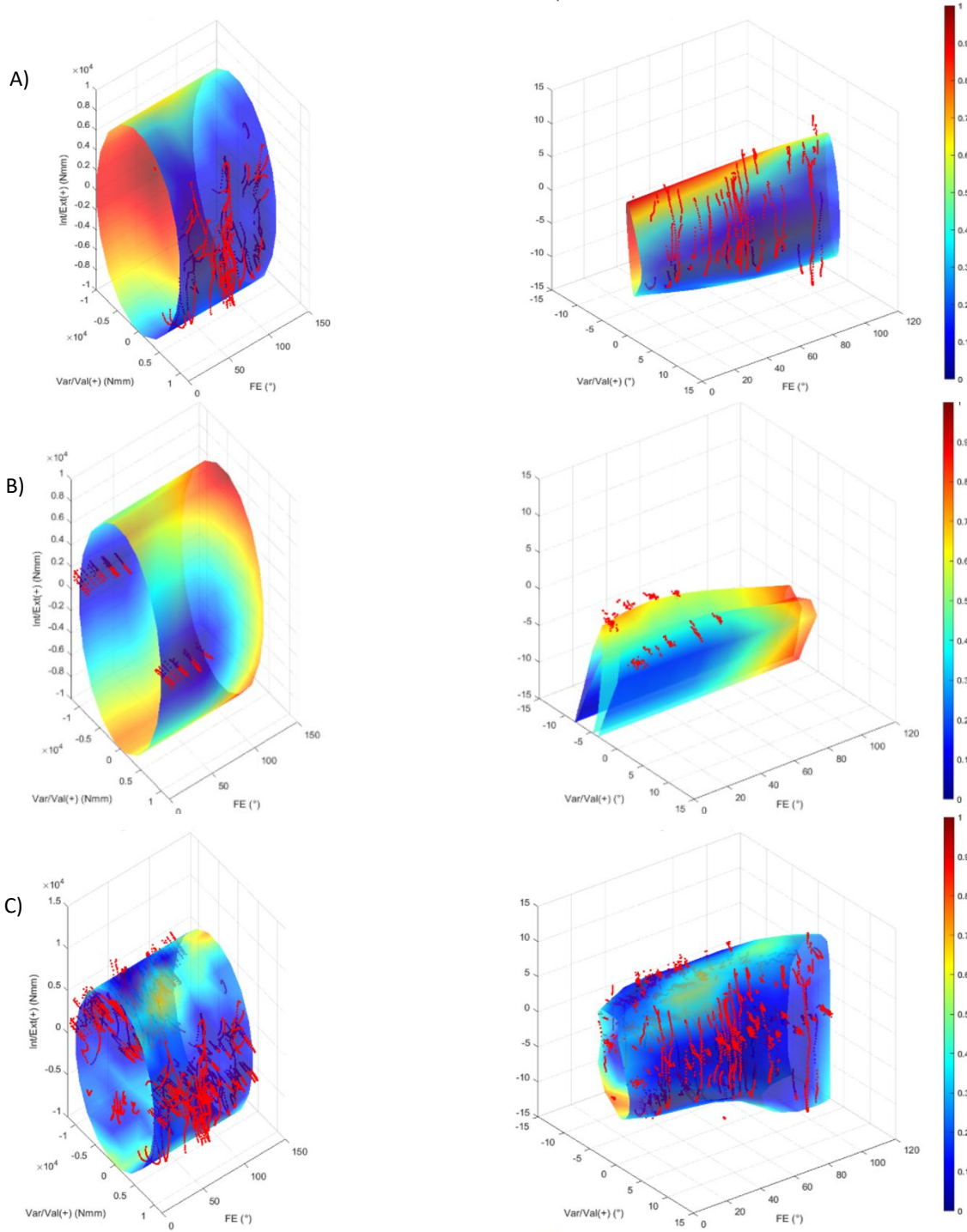
Fig. 13: The proposed feedback system showing the Isoload as a surface of the left and the development of the prediction as the surface on the right. The red points show what experimental points are collected that fall within the range of the desired isoload. The color of the surface is a representation of the data close to the desired location, with blue showing points that are close, (Plots A) are showing the feedback near the start of the envelope collection process using a new manipulation process. (Plots B) are showing the

feedback near the start of the envelope collection process using the traditional manipulation procedure. (Plots C) are showing the feedback near the end of the envelope collection process, showing the end results of both manipulations.
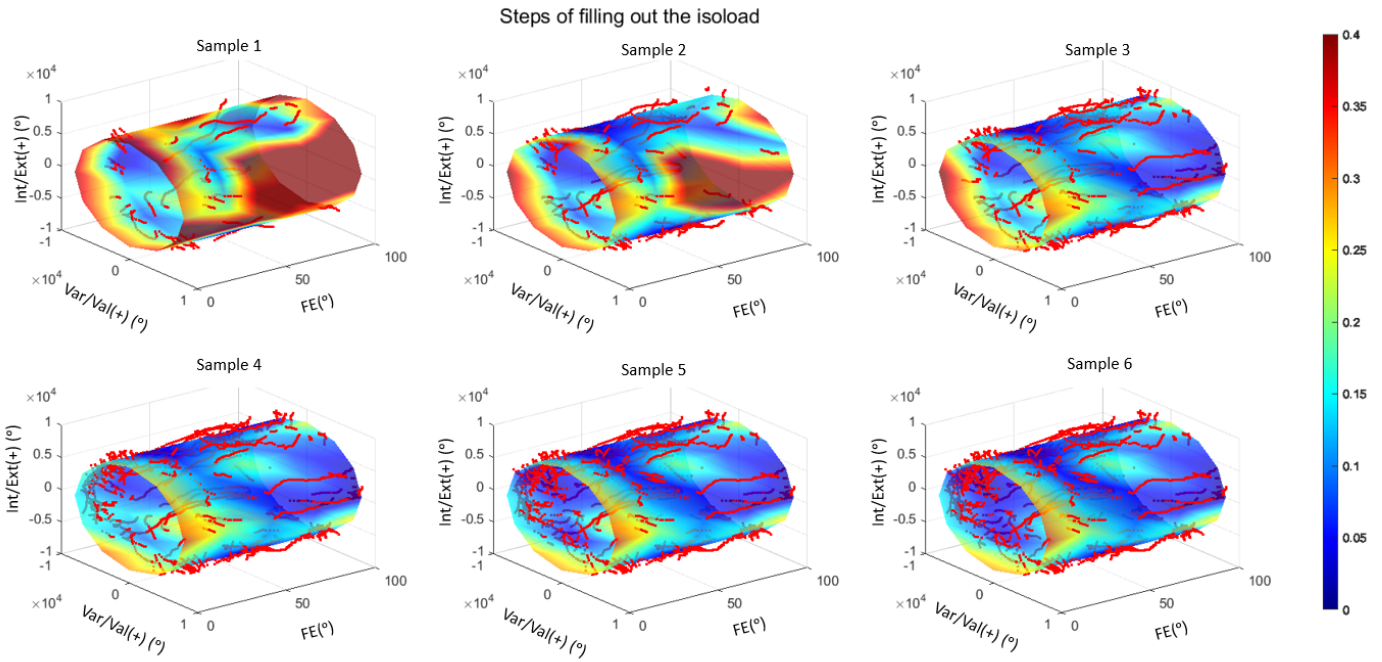

Fig. 14: Development of filling out the isoload surface of the feedback screen takes at six points across the collection process. The red is points where more data is needed, and blue is where they have enough data.
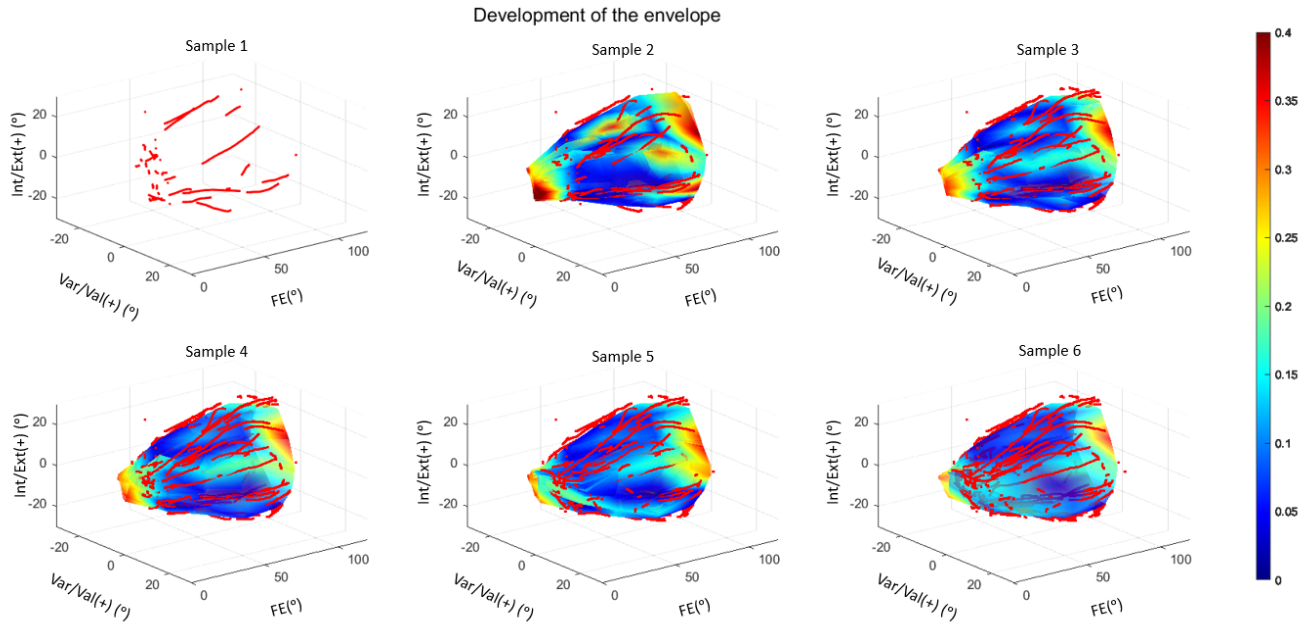
Fig. 15: Development of an envelope prediction on the feedback screen taken at six points across the collection process. The red shows points where more data is needed, and blue shows points that have enough data.
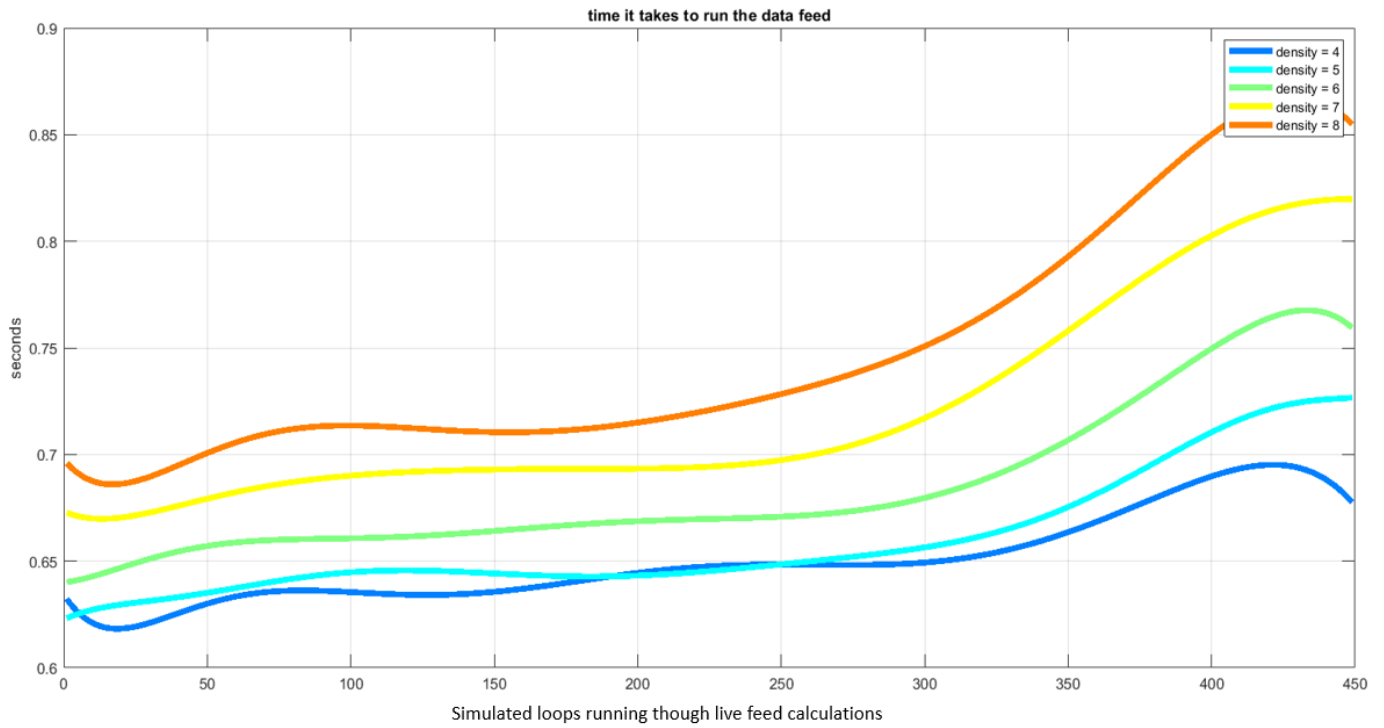
Fig. 16: Data feed run time based on surface density mesh. This test is done post experimentation, where the time required to calculate everything in that loop is displayed. The different colors show the time it takes to calculate the predictions based on the density of the surface mesh.
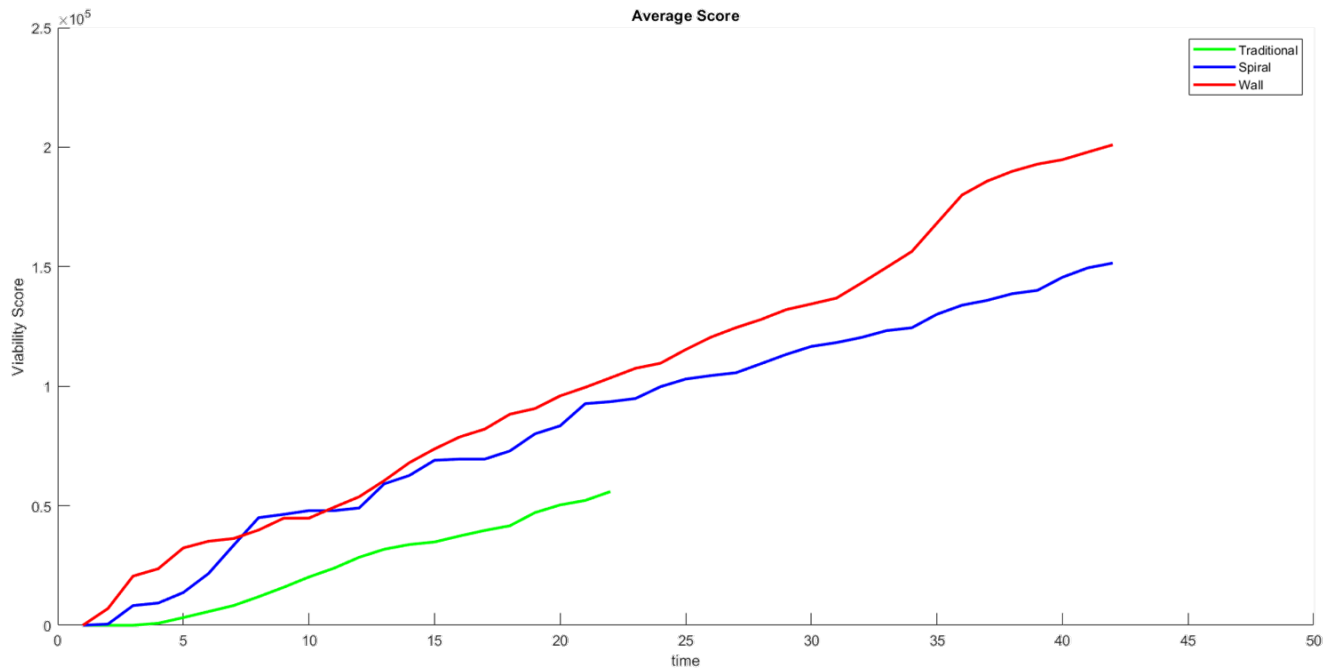

Fig. 17: Showing how the score changes over data collection. Both spiral and wall method consistently have a higher quality score at 10,000 Nmm isoload.

Chapter 4: Conclusion

The Experimental Joint Biomechanics Research Laboratory, at the University of Kansas, previously created a novel method of finding the variation in a knee envelope using the RBF to create a prediction. This study builds upon this previous research by better understanding a major cause of the variations in those predictions and generates an envelope quality score to help investigators understand if the quantity and distribution of data around specific isoloads will be able to generate a viable knee envelope. It also proposes a new feedback system to help investigators collect data around a target isoload and give them a new ability to make real time changes to data collection around the desired prediction, avoiding the over collection of data at lower loads where the lab is not as interested in observing. By producing a live feedback of the envelope development that displays where additional load data need to be taken during the current trial, it will guide researchers to collect data more efficiently and effectively to provide the RBF with a high enough quantity and distribution of experimental data to generate a higher quality envelope.

Load and displacement data collected in the EJBR lab using the same protocol for manual manipulation of 13 freshly frozen cadaver knees was analyzed using a sequential down sampling process to feed an RBF function to produce a passive knee envelope prediction for each of the 13 knees. This analysis allowed the comparison of areas of consistently higher variability in the resulting envelopes, and helped determine if changes could be made to achieve more efficient results with less variation. Because the radial basis function weights experimental points that are closer to the interpolated position more heavily than points that are further away, an envelope quality score could be assigned to a given data set by analyzing the distance, quantity, and distribution of experimental data points relative to the desired isoload. This score can guide

investigators at what isoload there is enough data to have confidence in their knee envelope prediction.

In addition to providing better ways to analyze previously collected data sets, this study aimed at helping investigators proactively collect new data points more efficiently and effectively to provide the RBF with a high enough quantity and distribution of experimental data to generate a higher quality envelope. The new feedback system shows investigators how to proactively manipulate the knee during data collection based on developing Matlab plots of the envelope prediction showing which data points fall close to the desired isoload, and the developing envelope prediction. This feedback screen is color coded and highlights where additional data points are needed to get the appropriate data for the desired prediction. The COVID pandemic forced the EJBRL shutdown during the later stages of this research, and because the primary investigator had moved from the University of Kansas by that time, the final testing of the new investigator feedback screen had to be done virtually in collaboration with an on campus investigator using Microsoft Teams. One investigator at KU fed data for the test of the three data collection methods online to the lead investigator, who had the Matlab code set up on another computer and ran the data sets live, producing and testing the new feedback display and giving live instruction to the on campus investigator, who collected the data. Also, because no cadaver knees were available for this one test due to the pandemic shutdown, a prosthetic knee was used. Because this particular test was focused on the investigator feedback display and the efficiency of the data collection, not the knee envelope itself, this did not affect or change any of the data or calculations used for Objective 1 or Objective 2. It was adequate for Objective 3, which was to confirm the effectiveness of the new investigator feedback system and to compare the efficiency of the three different data collection methods.   Future studies may be

able to also build in a calculation of the best envelopes that could be generated from the data

being currently collected.

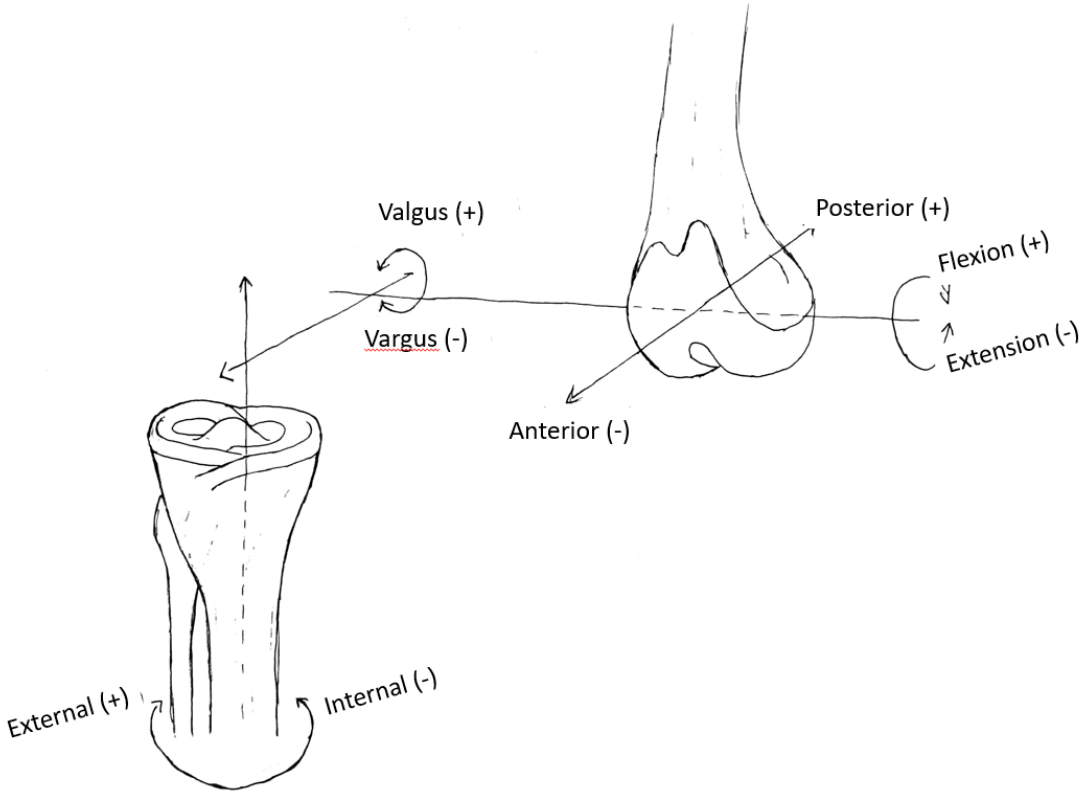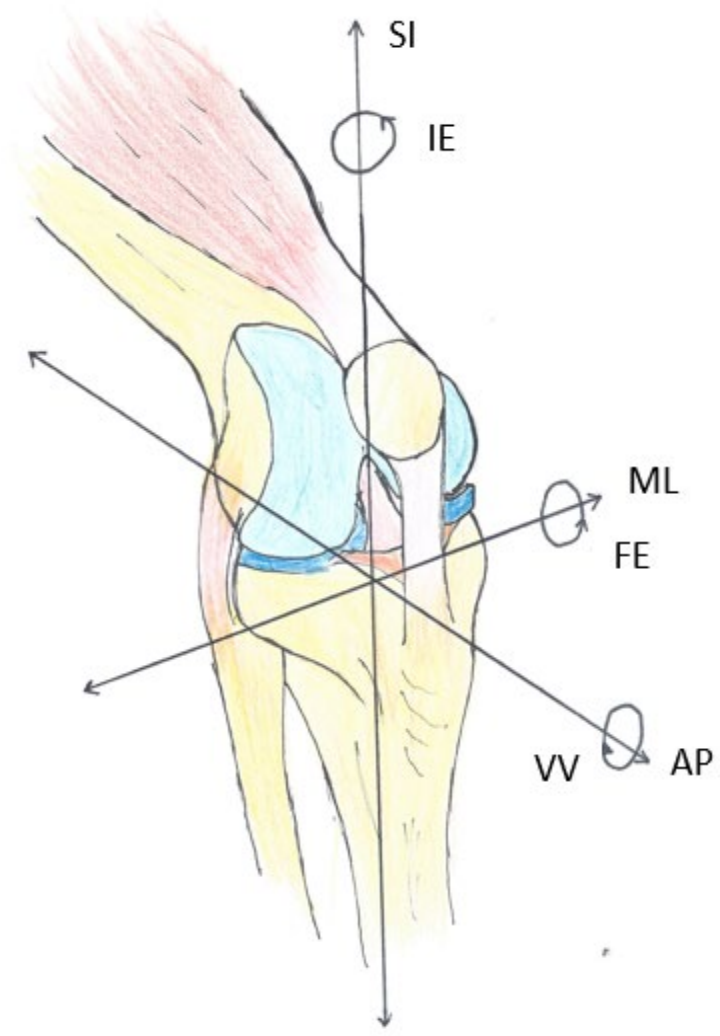# Appendix A: 6 Degrees of Freedom and Axes Images

Figure A.1 Another representation of the 6 degrees of freedom shown previously in Fig. 18. Superior/Inferior and Medial/Lateral translations are not labeled but axes are present.

Note: This is a right knee

Figure A2 Axes of the knee
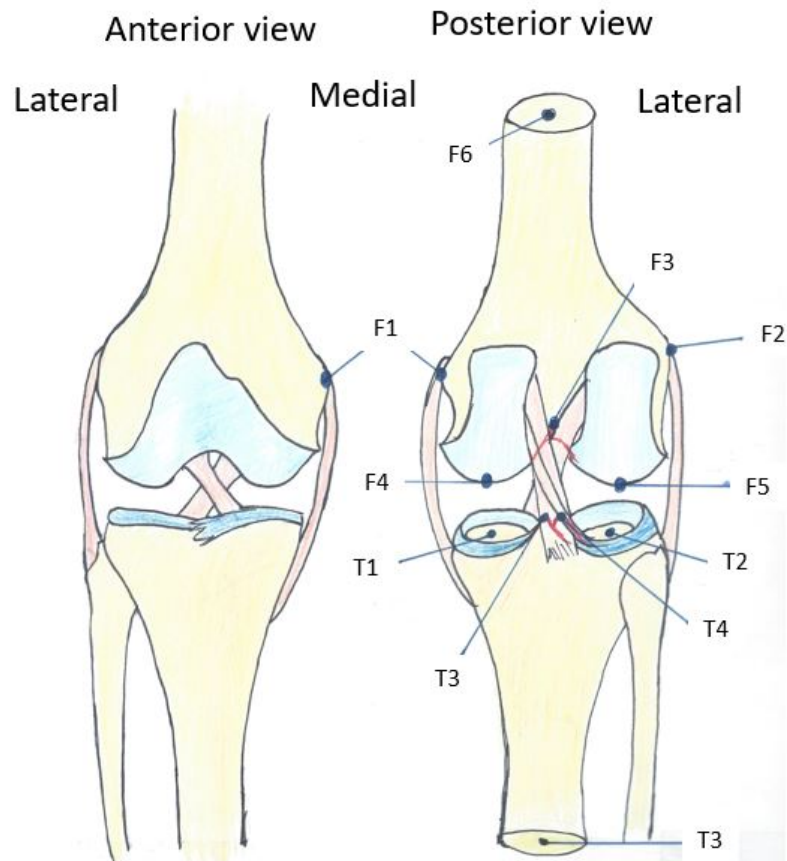
Appendix B: Probe Point locations

Figure B1: This is a representation of where the probe points are taken on the knee. It is important to get a good visualization of these probe points or else it can skew the results in an unwanted manner. Fortunately, we are able to have checkpoints throughout the data calculation process that allows a visualization of any error in taking the GS points.

FEMUR BONE POINTS	
F1	Medial Epicondyle
F2	Lateral Epicondyle
F3	Most Distal Point Between condyles
F4	Posterior Edge of Medial Condyle
F5	Posterior Edge of Lateral Condyle
F6	Bone end
TIBIA BONE POINTS	
T1	Center of Medial Plateau
T2	Center of Lateral Plateau
T3	Proximal Tip of the medial spine of the Tibial Eminence
T4	Proximal Tip of Tibial Intercondylar Notch
T5	Center of Ankle

Appendix C: MATLAB Code for New Investigator Feedback Screen

This code starts by clearing all displays and data in the program. Then it asks the investigator what experimental data they would like to import into the program. The investigator needs to tell the program what isoload they are studying. The program then cuts any experimental values that fall out of the range of the isoload, for example 10000 Nmm plus or minus 500Nmm range. That experimental data is then displayed on the isoload surface, which is color coded to tell the investigator where they need to collect more data based on the load. Then the experimental data is run through an RBF to generate an isoload prediction surface, and is color coded to tell the investigator where more data need to be collected based on position. This code displays the predictions on a figure that takes 6 snap shots of both surfaces, as well as generates a gif of the progression of the development of the envelope.

```
clc; clear all; close all; % Clears and closes everything for a new start of the program

set(0,'DefaultFigureWindowStyle','docked'); %docks the display in the matlab window (optional)

warning off;

cdur=cd; %sets the current directory of the file path


%% input values

%max loads

LoadVV=10000;

LoadIE=10000;

%cannot be the same number

FEmin=0; %starting flexion location

FEmax=100; % ending flexion location

%first and last .xls loop that is being fed into the program

%this is the experimental data file

first =1;

last=5;

%average points in find distance

n=10;

%+- what range around the isoload

ABrange=500;
```

```matlab
%leave this the same or it will be making a prediction based on a different

%isoload

isovalue=1;

% normal values

input=[7 2 3 5]; %these are the columns being input into the program,

%  col 7 is FE, col 2 is VV, col 3 is IE, col 5 is AP

output=[8 9 11]; output the data in the location of these col

% range of data, could be used to make a loop

%     FE    VV   IE   AP

range=[FEmin -LoadVV -LoadIE -100;   % minimums

   FEmax  LoadVV  LoadIE  100];    % maximums`


trials{1}=first:last;

%tells the investigator where the experimental data is located

cd([cdur '\Functions']);%move to this directory

[EXP,load,kin]=Get_EXP(trials,cdur);% get the data

cd([cdur]);%move back to the old directory

%this is the start of the loop that lets the investigator compare the density of the predicted mesh

%data skip, how much data do you want to use in the program if all data leave as 1

for Dskip=1

%    EXP=EXP(1:Dskip:end,:);

%this is the start of the loop that lets the investigator compare the density of the predicted mesh

%if you don't want to have this, leave a single value

  for denchange=5

     density=[denchange  denchange denchange 3];

% generates variable

     farloop=[];

     VP=[];

     FP=[];

     Ltime=[];

     Lvvposload=[]; %vv positive load

     Lvvnegload=[];%vv negative load

     TptsIN=[]; %total points in
```

```
SaveptsIN=[]; % save the points in for next loop

DataP=[];

loops=1;%starting loop value

LptsIN=[];% point in the current loop

FEloop=linspace(FEmin,FEmax,density(1));% equal distance through flexion extension based on the mesh
density you want


%this loop simulates the time aspect of collecting the data when data was collected previously before running the
code rather than using the code in real time

for time=1:100:length(EXP)%1:100:length(EXP)

        tic

%this is the first run of the loop

        if time ==1

            %           tic

            %make the grids

            a_plot=linspace(range(1),range(2),density(1));

            b_plot=linspace(range(3),range(4),density(2));

            c_plot=linspace(range(5),range(6),density(3));

            d_plot=linspace(range(7),range(8),density(4));

            [a_mesh,b_mesh,c_mesh,d_mesh]=ndgrid(a_plot,b_plot,c_plot,d_plot);


            %make the RBF grids

            loadcolumns=[reshape(a_mesh,[],1) reshape(b_mesh,[],1) reshape(c_mesh,[],1) reshape(d_mesh,[],1)];

            FullLoads = [max(abs(loadcolumns(:,2))) max(abs(loadcolumns(:,3))) max(abs(loadcolumns(:,4)))];


            %reshaped to create values in isovalues

            flex=length(unique(loadcolumns(:,1))); % how many unique flexion

            vv=length(unique(loadcolumns(:,2))); % how many unique vv load

            ie=length(unique(loadcolumns(:,3))); % how many unique ie load

            flex1=reshape(loadcolumns(:,1),flex,vv,[]); % reshape flexion

            vv2=reshape(loadcolumns(:,2),flex,vv,[]); % reshape vv Load

            ie2=reshape(loadcolumns(:,3),flex,vv,[]); % reshape ie Load

            e=sqrt(sum((loadcolumns(:,2:4)./FullLoads).^2,2));

            E=reshape(e,flex,vv,[]);
```

```matlab
        [f2,v2] = isosurface(flex1,vv2,ie2,E,isovalue(1));

        %convert to polar to find the ranges

        [theta,rho] = cart2pol(v2(:,2),v2(:,3));

        rhoMX=max(rho);

    Else
%this is starting the rest of the loops, basically this is what is generating the display for the investigator to use

        %% See if the data falls within the loop loads


        loopexp=EXP(Ltime:Dskip:time,:);

        [~,rho2] = cart2pol(loopexp(:,2),loopexp(:,3));

        dist=abs(rhoMX-rho2);

        [r,~]=find(dist>=-ABrange & dist<ABrange);

        ptsIN_first=loopexp(r,:);

        [r,c]=find(ptsIN_first(:,7)>=range(1) & ptsIN_first(:,7)<range(2));

        ptsIN=ptsIN_first(r,:);


        disp('got points in')

        %%
%if  there were no data point found during that data collection interval this tells the program to skip calculations
so it does not produce an error

        if isempty(TptsIN)

            if isempty(ptsIN)

            else

                TptsIN=ptsIN;

            end

            else

            if isempty(ptsIN)

            else

                TptsIN=[TptsIN;ptsIN];

            end

            B=TptsIN(:,[7 2 3]);


            norm_B = [(B(:,1) - min(v2(:,1))) / ( max(v2(:,1)) - min( v2(:,1)) ) (B(:,2) - min(v2(:,2))) / ( max(v2(:,2)) -
min(v2(:,2)) )  (B(:,3) - min(v2(:,3))) / ( max(v2(:,3)) - min(v2(:,3)) )]; %find the normal value of B
```

```matlab
        norm_v2 = [(v2(:,1) - min(v2(:,1))) / ( max(v2(:,1)) - min(v2(:,1)) ) (v2(:,2) - min(v2(:,2))) / ( max(v2(:,2)) -
min(v2(:,2)) )  (v2(:,3) - min(v2(:,3))) / ( max(v2(:,3)) - min(v2(:,3)) )]; %find the normal value of v2


        for dd=1:length(norm_v2)
            D2 = vecnorm(norm_v2(dd,:) - norm_B, 2, 2);
            D2_sorted=sort(D2);
%if the length of the points is greater than n, it will take n average points else it will take the distance of all points
            if length(D2_sorted)>=n


               D3(dd,:)=mean(D2_sorted(1:n,:));%finds the average distance of the surface to the points
            else
               D3(dd,:)=mean(D2_sorted);
            end
        end
        norm_D3=(D3(:,1) - min(D3(:,1))) / ( max(D3(:,1)) - min( D3(:,1)) );


        %% make the prediction


        if isempty(TptsIN)%if there are no experimental data points in range don't do calculations and cause
errors
        else
          if isempty(LptsIN)
             LptsIN=ptsIN;
          else
             LptsIN=[LptsIN; ptsIN];
          end
          runEnv=LptsIN;
          runEnv(find(isnan(runEnv*zeros(size(runEnv,2),1))),:)=[];
          runEnv = unique(runEnv,'rows');


          %% RBF
          %%Gather data, remove rows with NaN, and remove duplicate rows
          Scale = prctile(runEnv(:,input),[2.5 97.5]);
          Scale = Scale(2,:)-Scale(1,:);
```

```
%%Downsize for speed/RAM
runEnv = runEnv(1:4:end,:);


%%Get RBF centers scaled appropriately
Xcenters = [runEnv(:,input(1))/Scale(1) runEnv(:,input(2))/Scale(2) runEnv(:,input(3))/Scale(3)];%
runEnv(:,input(4))/Scale(4)];
Ycenters = runEnv(:,output);


%%Calculate Distances
phi = zeros(size(Xcenters,1));
for i=1:size(Xcenters,1)
    phi(:,i)=sqrt(sum((repmat(Xcenters(i,:),size(Xcenters,1),1)-Xcenters(:,:)).^2,2));
end
%%Calculate Weights
Weights=phi\Ycenters;


%% make mesh
%full mesh made
a_plot=linspace(range(1),range(2),density(1));
b_plot=linspace(range(3),range(4),density(2));
c_plot=linspace(range(5),range(6),density(3));
d_plot=linspace(range(7),range(8),density(4));
[a_mesh,b_mesh,c_mesh,d_mesh]=ndgrid(a_plot,b_plot,c_plot,d_plot);
Data1=[reshape(a_mesh,[],1) reshape(b_mesh,[],1) reshape(c_mesh,[],1)];% reshape(d_mesh,[],1)];
Data1=[Data1 zeros(size(Data1,1),3)];
X_plot = [Data1(:,1)/Scale(1) Data1(:,2)/Scale(2) Data1(:,3)/Scale(3)];% Data1(:,4)/Scale(4)];
%this is the loop that give the predicted distance based on the grid
%it fills is out first row vv dist ie dist ap dist then row two
for i=1:size(X_plot,1)
    phi=(sqrt(sum((repmat(X_plot(i,:),size(Xcenters,1),1)-Xcenters(:,:)).^2,2)))';  % distance from point
Xc to X
    for j=1:size(Weights,2)
        Data1(i,j+4)=phi*Weights(:,j);
```

```matlab
        end
    end
    flex1=reshape(Data1(:,1),flex,vv,[]); % reshape flexion
    vv1=reshape(Data1(:,5),flex,vv,[]); % reshape vv position
    ie1=reshape(Data1(:,6),flex,vv,[]); % reshape ie position



    [f3,v3] = isosurface(flex1,vv1,ie1,E,1);% % generates the surface
    disp('found RBF')
    %%
%repeate for the predicted surface
    B=TptsIN(:,[7 8 9]);
    norm_B = [(B(:,1) - min(v3(:,1))) / ( max(v3(:,1)) - min( v3(:,1)) ) (B(:,2) - min(v3(:,2))) / ( max(v3(:,2)) -
min(v3(:,2)) )  (B(:,3) - min(v3(:,3))) / ( max(v3(:,3)) - min(v3(:,3)) )];
    norm_v3 = [(v3(:,1) - min(v3(:,1))) / ( max(v3(:,1)) - min(v3(:,1)) ) (v3(:,2) - min(v3(:,2))) / ( max(v3(:,2))
- min(v3(:,2)) )  (v3(:,3) - min(v3(:,3))) / ( max(v3(:,3)) - min(v3(:,3)) )];
    for dd=1:length(norm_v3)
        D4 = vecnorm(norm_v3(dd,:) - norm_B, 2, 2);
        D4_sorted=sort(D4);
        if length(D2_sorted)>=n
            D5(dd,:)=mean(D4_sorted(1:n,:));
        else
            D5(dd,:)=mean(D4_sorted);
        end
    end
    norm_D7=(D5(:,1) - min(D5(:,1))) / ( max(D5(:,1)) - min( D5(:,1)) );
    end
    %% Plot
%displays the the predictions
    %  figure(loops)
    figure(4)
    subplot(1,3,1)
    hold on; grid on;
    if isempty(TptsIN)
```

```matlab
            pat=patch('Faces',f2,'Vertices',v2);
        else
```

% applies a patch or a skin of the predicted surface so the investigator is able to see the surface, f2 is the isoload faces v2 is the isoload vertices , 'FaceVertexCData' displays the next matrix as the color of the surface, then interprets the face color, remove the edges so it looks nice, and remove the lighting so the shading of the surface does not confuse the investigator during data collection

```matlab
pat=patch('Faces',f2,'Vertices',v2,'FaceVertexCData',norm_D3,'FaceColor','interp','EdgeColor','none','FaceLighting',
'none');
            hold on
            plot3(TptsIN(:,7),TptsIN(:,2),TptsIN(:,3),'r.') %also display the experimental data point
        end


        hold on;
```

%more setting to make the plot look better and easier to understand

```matlab
        set(gca,'YDir','reverse');alpha(pat,0.7);camlight('headlight');
        view(3);
```

%set the colorbar the colorbar title and location

```matlab
        cb = colorbar; colormap(jet);%cb.Label.String = 'average distance of ten points closest to the surface';
        set(cb, 'Position', [.95 .11 .01 .8150])
        caxis([0 0.4])
```

%label the axis

```matlab
        xlabel('FE (°)'); ylabel('Var/Val(+) (Nmm)'); zlabel('Int/Ext(+) (Nmm)')
        %        title(['average distance to points' num2str(mean(D3))])
        sgtitle(['Live Feed of the Load data and RBF predictions'  ])


        %% new plot with both showing the load and prediction
```

%repeat, depending on if you want still images or the gif,

```matlab
        % figure(loops)
        figure(4)
        subplot(1,2,2)
        hold on; grid on;
        if isempty(TptsIN)
```

```
else

    if isempty(runEnv)

    else

pat=patch('Faces',f3,'Vertices',v3,'FaceVertexCData',norm_D7,'FaceColor','interp','EdgeColor','none','FaceLighting',
'none');% displays the isosurface

        hold on

    end

    scatter3(TptsIN(:,7),TptsIN(:,8),TptsIN(:,9),'r.')%experimental data

    end

    hold on;
%make it readable

    view(3);

    set(gca,'YDir','reverse');alpha(pat,0.7);camlight('headlight');

    xlabel('FE (°)'); ylabel('Var/Val(+) (°)'); %zlabel('Int/Ext(+) (°)')

    cb = colorbar; colormap(jet);%cb.Label.String = 'average distance of ten points closest to the surface ';

    set(cb, 'Position', [.95 .11 .01 .8150])

    caxis([0 0.4 ])

    axis([0 120 -30 30 -30 30])


    %%

    %this is creating a gif of the loop and progression of the envelope

    if loops==1% && cuts==1

        gif(['side_by_side_' num2str(denchange)
'_density_grid.gif'],'DelayTime',0.2,'LoopCount',5,'frame',gcf)

    else

        gif

    end

    clf


    T(loops,denchange)=toc;

    T2(loops,Dskip)=T(loops,denchange);

    loops=loops+1;

    %%
```

```matlab
PMval=700;

bopexp=EXP(1:time,:);

if length(bopexp)>=(length(EXP)/6)-PMval & length(bopexp)<=(length(EXP)/6)+PMval

subpos=1;

%%

figure(1)

subplot(2,3,subpos)

hold on; grid on;

if isempty(TptsIN)

    pat=patch('Faces',f2,'Vertices',v2);

else


pat=patch('Faces',f2,'Vertices',v2,'FaceVertexCData',norm_D3,'FaceColor','interp','EdgeColor','none','FaceLighting',
'none');%

    hold on

    plot3(TptsIN(:,7),TptsIN(:,2),TptsIN(:,3),'r.')

end

hold on;

set(gca,'YDir','reverse');alpha(pat,0.7);camlight('headlight');

view(3);

cb = colorbar; colormap(jet);%cb.Label.String = 'average distance of ten points closest to the surface';

set(cb, 'Position', [.95 .11 .01 .8150])

caxis([0 0.4 ])

%    xlabel('FE (°)'); ylabel('Var/Val(+) (Nmm)'); zlabel('Int/Ext(+) (Nmm)')

title(['number data points' num2str(length(bopexp))])

sgtitle(['Steps of filling out the isoload'  ])


%%

figure(2)

subplot(2,3,subpos)

hold on; grid on;

if isempty(TptsIN)


else
```

```
            if isempty(runEnv)
            else
                if length(runEnv)>1
                else

pat=patch('Faces',f3,'Vertices',v3,'FaceVertexCData',norm_D7,'FaceColor','interp','EdgeColor','none','FaceLighting',
'none');%

                end
                hold on


            end
            scatter3(TptsIN(:,7),TptsIN(:,8),TptsIN(:,9),'r.')
        end


        hold on;
        view(3);
        set(gca,'YDir','reverse');alpha(pat,0.7);camlight('headlight');
        %    xlabel('FE (°)'); ylabel('Var/Val(+) (°)'); %zlabel('Int/Ext(+) (°)')
        cb = colorbar; colormap(jet);%cb.Label.String = 'average distance of ten points closest to the surface ';
        set(cb, 'Position', [.95 .11 .01 .8150])
        caxis([0 0.4 ])
        axis([0 120 -30 30 -30 30])
        title(['number data points' num2str(length(bopexp))])
        sgtitle(['Development of the envelope'  ])

    elseif length(bopexp)>=(length(EXP)/6)*2-PMval & length(bopexp)<=(length(EXP)/6)*2+PMval
        subpos=2;
        figure(1)
        subplot(2,3,subpos)
        hold on; grid on;
        if isempty(TptsIN)
            pat=patch('Faces',f2,'Vertices',v2);
        else
```

54

```
pat=patch('Faces',f2,'Vertices',v2,'FaceVertexCData',norm_D3,'FaceColor','interp','EdgeColor','none','FaceLighting',
'none');%

            hold on

            plot3(TptsIN(:,7),TptsIN(:,2),TptsIN(:,3),'r.')

        end


        hold on;

        set(gca,'YDir','reverse');alpha(pat,0.7);camlight('headlight');

        view(3);

        cb = colorbar; colormap(jet);%cb.Label.String = 'average distance of ten points closest to the surface';

        set(cb, 'Position', [.95 .11 .01 .8150])

        caxis([0 0.4 ])

        %    xlabel('FE (°)'); ylabel('Var/Val(+) (Nmm)'); zlabel('Int/Ext(+) (Nmm)')

        title(['number data points' num2str(length(bopexp))])

        sgtitle(['Steps of filling out the isoload'  ])

        %%

        figure(2)

        subplot(2,3,subpos)

        hold on; grid on;

        if isempty(TptsIN)


        else

            if isempty(runEnv)

            else

pat=patch('Faces',f3,'Vertices',v3,'FaceVertexCData',norm_D7,'FaceColor','interp','EdgeColor','none','FaceLighting',
'none');%

                 hold on

            end

            scatter3(TptsIN(:,7),TptsIN(:,8),TptsIN(:,9),'r.')

        end


        hold on;
```

```matlab
        view(3);

        set(gca,'YDir','reverse');alpha(pat,0.7);camlight('headlight');

%       xlabel('FE (°)'); ylabel('Var/Val(+) (°)'); %zlabel('Int/Ext(+) (°)')

        cb = colorbar; colormap(jet);%cb.Label.String = 'average distance of ten points closest to the surface ';

        set(cb, 'Position', [.95 .11 .01 .8150])

        caxis([0 0.4 ])

        axis([0 120 -30 30 -30 30])

        title(['number data points' num2str(length(bopexp))])

        sgtitle(['Development of the envelope'  ])


    elseif length(bopexp)>=(length(EXP)/6)*3-PMval & length(bopexp)<=(length(EXP)/6)*3+PMval
        subpos=3;
        figure(1)
        subplot(2,3,subpos)
        hold on; grid on;
        if isempty(TptsIN)
            pat=patch('Faces',f2,'Vertices',v2);
        else

pat=patch('Faces',f2,'Vertices',v2,'FaceVertexCData',norm_D3,'FaceColor','interp','EdgeColor','none','FaceLighting',
'none');%

            hold on
            plot3(TptsIN(:,7),TptsIN(:,2),TptsIN(:,3),'r.')
        end


        hold on;

        set(gca,'YDir','reverse');alpha(pat,0.7);camlight('headlight');

        view(3);

        cb = colorbar; colormap(jet);%cb.Label.String = 'average distance of ten points closest to the surface';

        set(cb, 'Position', [.95 .11 .01 .8150])

        caxis([0 0.4 ])

%       xlabel('FE (°)'); ylabel('Var/Val(+) (Nmm)'); zlabel('Int/Ext(+) (Nmm)')

        title(['number data points' num2str(length(bopexp))])

        sgtitle(['Steps of filling out the isoload'  ])
```

56

```matlab
%%
figure(2)
subplot(2,3,subpos)
hold on; grid on;
if isempty(TptsIN)
else
    if isempty(runEnv)
    else
pat=patch('Faces',f3,'Vertices',v3,'FaceVertexCData',norm_D7,'FaceColor','interp','EdgeColor','none','FaceLighting',
'none');%
        hold on
    end
    scatter3(TptsIN(:,7),TptsIN(:,8),TptsIN(:,9),'r.')
end
hold on;
view(3);
set(gca,'YDir','reverse');alpha(pat,0.7);camlight('headlight');
%    xlabel('FE (°)'); ylabel('Var/Val(+) (°)'); %zlabel('Int/Ext(+) (°)')
cb = colorbar; colormap(jet);%cb.Label.String = 'average distance of ten points closest to the surface ';
set(cb, 'Position', [.95 .11 .01 .8150])
caxis([0 0.4 ])
axis([0 120 -30 30 -30 30])
title(['number data points' num2str(length(bopexp))])
sgtitle(['Development of the envelope'  ])


elseif length(bopexp)>=(length(EXP)/6)*4-PMval & length(bopexp)<=(length(EXP)/6)*4+PMval
    subpos=4;
    figure(1)
    subplot(2,3,subpos)
    hold on; grid on;
    if isempty(TptsIN)
        pat=patch('Faces',f2,'Vertices',v2);
    else
```

```matlab
pat=patch('Faces',f2,'Vertices',v2,'FaceVertexCData',norm_D3,'FaceColor','interp','EdgeColor','none','FaceLighting',
'none');%

        hold on

        plot3(TptsIN(:,7),TptsIN(:,2),TptsIN(:,3),'r.')

    end


    hold on;

    set(gca,'YDir','reverse');alpha(pat,0.7);camlight('headlight');

    view(3);

    cb = colorbar; colormap(jet);%cb.Label.String = 'average distance of ten points closest to the surface';

    set(cb, 'Position', [.95 .11 .01 .8150])

    caxis([0 0.4 ])

    %    xlabel('FE (°)'); ylabel('Var/Val(+) (Nmm)'); zlabel('Int/Ext(+) (Nmm)')

    title(['number data points' num2str(length(bopexp))])

    sgtitle(['Steps of filling out the isoload'  ])

    %%

    figure(2)

    subplot(2,3,subpos)

    hold on; grid on;

    if isempty(TptsIN)


    else

        if isempty(runEnv)

        else

pat=patch('Faces',f3,'Vertices',v3,'FaceVertexCData',norm_D7,'FaceColor','interp','EdgeColor','none','FaceLighting',
'none');%

            hold on

        end

        scatter3(TptsIN(:,7),TptsIN(:,8),TptsIN(:,9),'r.')

    end


    hold on;
```

```matlab
view(3);
set(gca,'YDir','reverse');alpha(pat,0.7);camlight('headlight');
%    xlabel('FE (°)'); ylabel('Var/Val(+) (°)'); %zlabel('Int/Ext(+) (°)')
cb = colorbar; colormap(jet);%cb.Label.String = 'average distance of ten points closest to the surface ';
set(cb, 'Position', [.95 .11 .01 .8150])
caxis([0 0.4 ])
axis([0 120 -30 30 -30 30])
title(['number data points' num2str(length(bopexp))])
sgtitle(['Development of the envelope'  ])


elseif length(bopexp)>=(length(EXP)/6)*5-PMval & length(bopexp)<=(length(EXP)/6)*5+PMval
    subpos=5;
    figure(1)
    subplot(2,3,subpos)
    hold on; grid on;
    if isempty(TptsIN)
        pat=patch('Faces',f2,'Vertices',v2);
    else

pat=patch('Faces',f2,'Vertices',v2,'FaceVertexCData',norm_D3,'FaceColor','interp','EdgeColor','none','FaceLighting',
'none');%
        hold on
        plot3(TptsIN(:,7),TptsIN(:,2),TptsIN(:,3),'r.')
    end

    hold on;
    set(gca,'YDir','reverse');alpha(pat,0.7);camlight('headlight');
    view(3);
    cb = colorbar; colormap(jet);%cb.Label.String = 'average distance of ten points closest to the surface';
    set(cb, 'Position', [.95 .11 .01 .8150])
    caxis([0 0.4 ])
    %    xlabel('FE (°)'); ylabel('Var/Val(+) (Nmm)'); zlabel('Int/Ext(+) (Nmm)')
    title(['number data points' num2str(length(bopexp))])
    sgtitle(['Steps of filling out the isoload'  ])
```

```matlab
%%
figure(2)
subplot(2,3,subpos)
hold on; grid on;
if isempty(TptsIN)


else

    if isempty(runEnv)
    else

pat=patch('Faces',f3,'Vertices',v3,'FaceVertexCData',norm_D7,'FaceColor','interp','EdgeColor','none','FaceLighting',
'none');%

        hold on
    end
    scatter3(TptsIN(:,7),TptsIN(:,8),TptsIN(:,9),'r.')
end


hold on;
view(3);
set(gca,'YDir','reverse');alpha(pat,0.7);camlight('headlight');
%    xlabel('FE (°)'); ylabel('Var/Val(+) (°)'); %zlabel('Int/Ext(+) (°)')
cb = colorbar; colormap(jet);%cb.Label.String = 'average distance of ten points closest to the surface ';
set(cb, 'Position', [.95 .11 .01 .8150])
caxis([0 0.4 ])
axis([0 120 -30 30 -30 30])
title(['number data points' num2str(length(bopexp))])
sgtitle(['Development of the envelope'  ])

  elseif length(bopexp)>=(length(EXP)/6)*6-PMval & length(bopexp)<=(length(EXP)/6)*6+PMval
    subpos=6;
    figure(1)
    subplot(2,3,subpos)
    hold on; grid on;
    if isempty(TptsIN)
```

60

```matlab
                pat=patch('Faces',f2,'Vertices',v2);
           else

pat=patch('Faces',f2,'Vertices',v2,'FaceVertexCData',norm_D3,'FaceColor','interp','EdgeColor','none','FaceLighting',
'none');%
                hold on
                plot3(TptsIN(:,7),TptsIN(:,2),TptsIN(:,3),'r.')
           end


           hold on;
           set(gca,'YDir','reverse');alpha(pat,0.7);camlight('headlight');
           view(3);
           cb = colorbar; colormap(jet);%cb.Label.String = 'average distance of ten points closest to the surface';
           set(cb, 'Position', [.95 .11 .01 .8150])
           caxis([0 0.4 ])
           %     xlabel('FE (°)'); ylabel('Var/Val(+) (Nmm)'); zlabel('Int/Ext(+) (Nmm)')
           title(['number data points' num2str(length(bopexp))])
           sgtitle(['Steps of filling out the isoload'  ])
           %%
           figure(2)
           subplot(2,3,subpos)
           hold on; grid on;
           if isempty(TptsIN)

           else
              if isempty(runEnv)
              else

pat=patch('Faces',f3,'Vertices',v3,'FaceVertexCData',norm_D7,'FaceColor','interp','EdgeColor','none','FaceLighting',
'none');%
                   hold on
              end
              scatter3(TptsIN(:,7),TptsIN(:,8),TptsIN(:,9),'r.')
           end
```

```matlab
            hold on;

            view(3);

            set(gca,'YDir','reverse');alpha(pat,0.7);camlight('headlight');

            %    xlabel('FE (°)'); ylabel('Var/Val(+) (°)'); %zlabel('Int/Ext(+) (°)')

            cb = colorbar; colormap(jet);%cb.Label.String = 'average distance of ten points closest to the surface ';

            set(cb, 'Position', [.95 .11 .01 .8150])

            caxis([0 0.4 ])

            axis([0 120 -30 30 -30 30])

            title(['loop number' num2str(loops)])

            sgtitle(['Development of the envelope'  ])

        else

            disp('error')


        end

        end

        Ltime=time;


    end


    end


end
```

References

References

[1] L. Blankevoort, R. Huiskes, and A. de Lange, "The envelope of passive knee joint motion," *Journal of Biomechanics*, vol. 21, no. 9, pp. 705–720, 1988, doi: 10.1016/0021-9290(88)90280-1.

[2] S. Shalhoub *et al.*, "In Vitro Experimental Testing of the Human Knee: A Concise Review," *J Knee Surg*, vol. 29, no. 02, pp. 138–148, 2015, doi: 10.1055/s-0035-1566739.

[3] K. Jensen, "Literature Review: Manual Laxity Tests for Anterior Cruciate Ligament Injuries," *J Orthop Sports Phys Ther*, vol. 11, no. 10, pp. 474–481, 1990, doi: 10.2519/jospt.1990.11.10.474.

[4] R. Rossi, F. Dettoni, M. Bruzzone, U. Cottino, D. G. D'Elicio, and D. E. Bonasia, "Clinical examination of the knee: know your tools for diagnosis of knee injuries," *BMC Sports Sci Med Rehabil*, vol. 3, no. 1, 2011, doi: 10.1186/1758-2555-3-25.

[5] J. Park and I. W. Sandberg, "Universal Approximation Using Radial-Basis-Function Networks," *Neural Computation*, vol. 3, no. 2, pp. 246–257, 1991, doi: 10.1162/neco.1991.3.2.246.

[6] F. G. Girgis, J. L. Marshall, and A. R. S. Al. MONA JEM, "The Cruciate Ligaments of the Knee Joint," *Clinical Orthopaedics and Related Research*, vol. 106, pp. 216–231, 1975, doi: 10.1097/00003086-197501000-00033.

[7] K. L. Markolf, A. Kochan, and H. C. Amstutz, "Measurement of knee stiffness and laxity in patients with documented absence of the anterior cruciate ligament.," *The Journal of Bone & Joint Surgery*, vol. 66, no. 2, pp. 242–252, 1984, doi: 10.2106/00004623-198466020-00011.

[8] H. Matsumoto and B. B. Seedhom, "Rotation of the Tibia in the Normal and Ligament-Deficient Knee. A study Using Biplanar Photography," *Proc Inst Mech Eng H*, vol. 207, no. 3, pp. 175–184, 1993, doi: 10.1243/pime_proc_1993_207_290_02.

[9] F. K. Fuss, "'Voluntary rotation in the human knee joint,'" vol. 179, no. vol. 179, pp. 115–125, 1991., J. Anat., pp. 115–125, 1991.

[10] A. Amis, A. M. J. Bull, C. M. Gupte, I. Hijazi, A. Race, and J. R. Robinson, "Biomechanics of the PCL and related structures: posterolateral, posteromedial and meniscofemoral ligaments," *Knee Surgery, Sports Traumatology, Arthroscopy*, vol. 11, no. 5, pp. 271–281, 2003, doi: 10.1007/s00167-003-0410-7.

[11] D. L. Gollehon, P. A. Torzilli, and R. F. Warren, "The role of the posterolateral and cruciate ligaments in the stability of the human knee. A biomechanical study.," *The Journal of Bone & Joint Surgery*, vol. 69, no. 2, pp. 233–242, 1987, doi: 10.2106/00004623-198769020-00010.

[12] A.B. Wymenga, J. J. Kats, J. Kooloos, and B. Hillen, "Surgical anatomy of the medial collateral ligament and the posteromedial capsule of the knee," *Knee Surg Sports Traumatol Arthrosc*, vol. 14, no. 3, pp. 229–234, 2006, doi: 10.1007/s00167-005-0682-1.

[13] A.R. Sanchez, M. T. Sugalski, and R. F. LaPrade, "Anatomy and Biomechanics of the Lateral Side of the Knee," *Sports Medicine and Arthroscopy Review*, vol. 14, no. 1, pp. 2–11, 2006, doi: 10.1097/00132585-200603000-00002.

[14] G. Niccoli, D. Mercurio, and F. Cortese, ""Bone scan in Painful knee arthroplasty: obsolete or actual examination?," *Acta Biomed,* vol. 88, pp. 68–77, doi: doi: 10.23750/abm.v88i2.

[15] S. G. F. Abram, A. J. Price, A. Judge, and D. J. Beard, "Anterior cruciate ligament (ACL) reconstruction and meniscal repair rates have both increased in the past 20 years in England: hospital statistics from 1997 to 2017," *Br J Sports Med*, vol. 54, no. 5, pp. 286–291, 2020, doi: 10.1136/bjsports-2018-100195.

[16] C. Levin, "Physical Examination of the Spine and Extremities," vol. 57, no. 10, pp. 1220–1220, 1977, doi: 10.1093/ptj/57.10.1220.

[17] R. L. Larson, "Physical Examination in the Diagnosis of Rotatory Instability," *Clinical Orthopaedics and Related Research*, vol. NA;, no. 172, p. 38???44, 1983, doi: 10.1097/00003086-198301000-00009.

[18] W. F. Donaldson, R. F. Warren, and T. Wickiewicz, "A comparison of acute anterior cruciate ligament examinations," *Am J Sports Med*, vol. 13, no. 1, pp. 5–10, 1985, doi: 10.1177/036354658501300102.

[19] J. S. Torg, W. Conrad, and V. Kalen, "Clinical I diagnosis of anterior cruciate ligament instability in the athlete," *Am J Sports Med*, vol. 4, no. 2, pp. 84–93, 1976, doi: 10.1177/036354657600400206.

[20] R. A. Gurtler, R. Stine, and J. S. TORG, "Lachman Test Evaluated," *Clinical Orthopaedics and Related Research*, vol. NA;, no. 216, p. 141–150, 1987, doi: 10.1097/00003086-198703000-00022.

[21] B. E. Kilinc, A. Kara, H. Celik, Y. Oc, and S. Camur, "Evaluation of the accuracy of Lachman and Anterior Drawer Tests with KT1000 ın the follow-up of anterior cruciate ligament surgery," *J Exerc Rehabil*, vol. 12, no. 4, pp. 363–367, 2016, doi: 10.12965//jer.1632622.311.

[22] L. S. Bickley, *Bates' Guide To Physical Examination and History Taking*. LWW, 2020.

[23] J. L. Long and J. E. Carpenter, "Medial Collateral Ligament Injury," *Essential Orthopaedics*, vol. 3, no. No. 1, pp. 620–623, 2010, doi: 10.1016/b978-1-4160-5473-3.00144-1.

[24] G. A. Malanga, S. Andrus, S. F. Nadler, and J. McLean, "Physical examination of the knee: A review of the original test description and scientific validity of common orthopedic tests," *Archives of Physical Medicine and Rehabilitation*, vol. 84, no. 4, pp. 592–603, 2003, doi: 10.1053/apmr.2003.50026.

[25] M. C. S. Inacio, S. E. Graves, N. L. Pratt, E. E. Roughead, and S. Nemes, "Increase in Total Joint Arthroplasty Projected from 2014 to 2046 in Australia: A Conservative Local Model With International Implications," *Clinical Orthopaedics and Related Research*, vol. 475, no. 8, pp. 2130–2137, 2017, doi: 10.1007/s11999-017-5377-7.

[26] J. C. Chow and L. Breslauer, "The Use of Intraoperative Sensors Significantly Increases the Patient-Reported Rate of Improvement in Primary Total Knee Arthroplasty," *Orthopedics*, vol. 40, no. 4, 2017, doi: 10.3928/01477447-20170503-01.

[27] K. A. Gustke, G. J. Golladay, M. W. Roche, L. C. Elson, and C. R. Anderson, "A Targeted Approach to Ligament Balancing Using Kinetic Sensors," *The Journal of Arthroplasty*, vol. 32, no. 7, pp. 2127–2132, 2017, doi: 10.1016/j.arth.2017.02.021.

[28] W. L. Jaffe, J. M. Dundon, and T. Camus, "Alignment and Balance Methods in Total Knee Arthroplasty," *Journal of the American Academy of Orthopaedic Surgeons*, vol. 26, no. 20, pp. 709–716, 2018, doi: 10.5435/jaaos-d-16-00428.

[29] L. C. Walker, N. D. Clement, K. M. Ghosh, and D. J. Deehan, "What is a balanced knee replacement?," *EFORT Open Reviews*, vol. 3, no. 12, pp. 614–619, 2018, doi: 10.1302/2058-5241.3.180008.

[30] T. K. Fehring, "Rotational Malalignment of the Femoral Component in Total Knee Arthroplasty," *Clinical Orthopaedics and Related Research*, vol. 380, pp. 72–79, 2000, doi: 10.1097/00003086-200011000-00010.

[31] M. A. Katz, T. D. Beck, J. S. Silber, R. M. Seldes, and P. A. Lotke, "Determining femoral rotational alignment in total knee arthroplasty," *The Journal of Arthroplasty*, vol. 16, no. 3, pp. 301–305, 2001, doi: 10.1054/arth.2001.21456.

[32] F. M. Griffin, J. N. Insall, and G. R. Scuderi, "Accuracy of soft tissue balancing in total knee arthroplasty," *The Journal of Arthroplasty*, vol. 15, no. 8, pp. 970–973, 2000, doi: 10.1054/arth.2000.6503.

[33] F. M. Griffin, K. Math, G. R. Scuderi, J. N. Insall, and P. L. Poilvache, "Anatomy of the epicondyles of the distal femur," *The Journal of Arthroplasty*, vol. 15, no. 3, pp. 354–359, 2000, doi: 10.1016/s0883-5403(00)90739-3.

[34] V. Kinzel, M. Ledger, and D. Shakespeare, "Can the epicondylar axis be defined accurately in total knee arthroplasty?," *The Knee*, vol. 12, no. 4, pp. 293–296, 2005, doi: 10.1016/j.knee.2004.09.003.

[35] J. Jerosch, E. Peuker, B. Philipps, and T. Filler, "Interindividual reproducibility in perioperative rotational alignment of femoral components in knee prosthetic surgery using the transepicondylar axis," *Knee, Surg, Sports Traumatol, Arthrosc*, vol. 10, no. 3, pp. 194–197, 2002, doi: 10.1007/s00167-001-0271-x.

[36] B. K. Daines and D. A. Dennis, "Gap Balancing vs. Measured Resection Technique in Total Knee Arthroplasty," *Clin Orthop Surg*, vol. 6, no. 1, p. 1, 2014, doi: 10.4055/cios.2014.6.1.1.

[37] G. J. Golladay *et al.*, "Are Patients More Satisfied With a Balanced Total Knee Arthroplasty?," *The Journal of Arthroplasty*, vol. 34, no. 7, pp. S195–S200, 2019, doi: 10.1016/j.arth.2019.03.036.

[38] K. Gromov, M. Korchi, M. G. Thomsen, H. Husted, and A. Troelsen, "What is the optimal alignment of the tibial and femoral components in knee arthroplasty?," *Acta Orthopaedica*, vol. 85, no. 5, pp. 480–487, 2014, doi: 10.3109/17453674.2014.940573.

[39] J. J. Cherian, B. H. Kapadia, S. Banerjee, J. J. Jauregui, K. Issa, and M. A. Mont, "Mechanical, Anatomical, and Kinematic Axis in TKA: Concepts and Practical

Applications," *Curr Rev Musculoskelet Med*, vol. 7, no. 2, pp. 89–95, 2014, doi: 10.1007/s12178-014-9218-y.

[40] S. M. Howell, "Kinematic Vs. Mechanical Alignment: What Is The Difference?," *Orthopedics Today*, 01-Oct-2010. [Online]. Available: https://www.healio.com/news/orthopedics/20120325/kinematic-vs-mechanical-alignment-what-is-the-difference. [Accessed: 09-Jun-2021].

[41] W. Blakeney, J. Clément, F. Desmeules, N. Hagemeister, C. Rivière, and P.-A. Vendittoli, "Kinematic alignment in total knee arthroplasty better reproduces normal gait than mechanical alignment," *Knee Surg Sports Traumatol Arthrosc*, vol. 27, no. 5, pp. 1410–1417, 2019, doi: 10.1007/s00167-018-5174-1.

[42] M. Hadi, T. Barlow, I. Ahmed, M. Dunbar, P. McCulloch, and D. Griffin, "Does malalignment affect revision rate in total knee replacements: a systematic review of the literature," *SpringerPlus*, vol. 4, no. 1, 2015, doi: 10.1186/s40064-015-1604-4.

[43] R. Seil and D. Pape, "Causes of failure and etiology of painful primary total knee arthroplasty," *Knee Surg Sports Traumatol Arthrosc*, vol. 19, no. 9, pp. 1418–1432, 2011, doi: 10.1007/s00167-011-1631-9.

[44] M. C. S. Inacio, E. W. Paxton, S. E. Graves, R. S. Namba, and S. Nemes, "Projected increase in total knee arthroplasty in the United States – an alternative projection model," *Osteoarthritis and Cartilage*, vol. 25, no. 11, pp. 1797–1803, 2017, doi: 10.1016/j.joca.2017.07.022.

[45] A.Liu, E. Ingham, J. Fisher, and L. M. Jennings, "Development of a pre-clinical experimental simulation model of the natural porcine knee with appropriate ligamentous constraints," *PLoS ONE*, vol. 14, no. 5, p. e0216872, 2019, doi: 10.1371/journal.pone.0216872.

[46] A.C. Bitar ., "Histological study of fresh versus frozen semitendinous muscle tendon allografts," *Clinics*, vol. 65, no. 3, 2010, doi: 10.1590/s1807-59322010000300010.

[47] J. Reinders, R. Sonntag, L. Vot, C. Gibney, M. Nowack, and J. P. Kretzer, "Wear Testing of Moderate Activities of Daily Living Using In Vivo Measured Knee Joint Loading," *PLoS ONE*, vol. 10, no. 3, p. e0123155, 2015, doi: 10.1371/journal.pone.0123155.

[48] J. P. Halloran, C. W. Clary, L. P. Maletsky, M. Taylor, A. J. Petrella, and P. J. Rullkoetter, "Verification of Predicted Knee Replacement Kinematics During Simulated Gait in the Kansas Knee Simulator," *Journal of Biomechanical Engineering*, vol. 132, no. 8, 2010, doi: 10.1115/1.4001678.

[49] J. D. Roth, S. M. Howell, and M. L. Hull, "Envelopes of Passive Motion in the Intact Tibiofemoral Joint: An In Vitro Study," *Student Paper and Design Competitions*, vol. 1B, no. Extremity; Fluid Mechanics; Gait; Growth, Remodeling, and Repair; Heart Valves; Injury Biomechanics; Mechanotransduction and Sub-Cellular Biophysics; MultiScale Biotransport; Muscle, Tendon and Ligament; Musculoskeletal Devices; Multiscale Mechanics; Thermal Medicine; Ocular Biomechanics; Pediatric Hemodynamics; Pericellular Phenomena; Tissue Mechanics; Biotransport Design and Devices; Spine;

Stent Device Hemodynamics; Vascular Solid Mechanics; Student Paper and Design Competitions, 2013, doi: 10.1115/sbc2013-14319.

[50] J. D. Roth, S. M. Howell, and M. L. Hull, "Analysis of differences in laxities and neutral positions from native after kinematically aligned TKA using cruciate retaining implants," *J. Orthop. Res.*, vol. 37, no. 2, pp. 358–369, 2019, doi: 10.1002/jor.24196.

[51] A. J. Cyr, S. S. Shalhoub, F. G. Fitzwater, L. A. Ferris, and L. P. Maletsky, "Mapping of Contributions From Collateral Ligaments to Overall Knee Joint Constraint: An Experimental Cadaveric Study," *Journal of Biomechanical Engineering*, vol. 137, no. 6, 2015, doi: 10.1115/1.4029980.

[52] G. Salvadore, P. A. Meere, M. A. Verstraete, J. Victor, and P. S. Walker, "Laxity and contact forces of total knee designed for anatomic motion: A cadaveric study," *The Knee*, vol. 25, no. 4, pp. 650–656, 2018, doi: 10.1016/j.knee.2018.04.014.

[53] K. M. Ghosh, A. P. Blain, L. Longstaff, S. Rushton, A. A. Amis, and D. J. Deehan, "Can we define envelope of laxity during navigated knee arthroplasty?," *Knee Surg Sports Traumatol Arthrosc*, vol. 22, no. 8, pp. 1736–1743, 2014, doi: 10.1007/s00167-013-2574-0.

[54] " NDI Measurement Sciences, "Optotrak Certus.," *NDI* . [Online]. Available: http://www.ndigital.com/msci/products/optotrak-certus/.

[55] L. P. Maletsky, J. Sun, and N. A. Morton, "Accuracy of an optical active-marker system to track the relative motion of rigid bodies," *Journal of Biomechanics*, vol. 40, no. 3, pp. 682–685, 2007, doi: 10.1016/j.jbiomech.2006.01.017.

[56] N. B. Schuler, M. J. Bey, J. T. Shearn, and D. L. Butler, "Evaluation of an electromagnetic position tracking device for measuring in vivo, dynamic joint kinematics," *Journal of Biomechanics*, vol. 38, no. 10, pp. 2113–2117, 2005, doi: 10.1016/j.jbiomech.2004.09.015.

[57] E. S. Grood and W. J. Suntay, "A Joint Coordinate System for the Clinical Description of Three-Dimensional Motions: Application to the Knee," *Journal of Biomechanical Engineering*, vol. 105, no. 2, pp. 136–144, 1983, doi: 10.1115/1.3138397.

[58] J. Cyr and L. P. Maletsky, "Technical note: a multi-dimensional description of knee laxity using radial basis functions," *Computer Methods in Biomechanics and Biomedical Engineering*, vol. 18, no. 15, pp. 1674–1679, 2015, doi: 10.1080/10255842.2014.946913.

[59] J. Lin, Y. Zhao, D. Watson, and C. S. Chen, "The radial basis function differential quadrature method with ghost points," *Mathematics and Computers in Simulation*, vol. 173, pp. 105–114, 2020, doi: 10.1016/j.matcom.2020.01.006.

[60] "A Novel Method for Quantifying Uncertainty in the Unified Envelope of Constraint in the Passive Knee Joint." M.S.Thesis, University of Kansas, 2018.

[61] "MIS Multi-Reference® 4-in-1 Femoral Instrumentation For NexGen® Cruciate Retaining & NexGen Legacy® Posterior Stabilized Knees Surgical Technique," *Zimmer Biomet website*. [Online]. Available: https://www.zimmerbiomet.com/content/dam/zimmer-biomet/medical-professionals/000-surgical-techniques/knee/1402.1-GLBL-en%20MIS%20Multi-Reference%204-in-1%20Femoral%20Instrumentation-Final.pdf. [Accessed: 08-Jun-2021].

[62] X. He, H. Cai, and K. Zhang, "Pie-crusting technique is effective and safe to release superficial medial collateral ligament for total knee arthroplasty," *Journal of Orthopaedic Translation*, vol. 13, pp. 33–40, 2018, doi: 10.1016/j.jot.2018.01.001.

[63] S. Babazadeh, "The relevance of ligament balancing in total knee arthroplasty: how important is it? A systematic review of the literature," *Orthop Rev (Pavia)*, vol. 1, no. 1, p. 26, 2009, doi: 10.4081/or.2009.e26.

[64] Z. C. Lum, A. K. Shieh, and L. D. Dorr, "Why total knees fail-A modern perspective review," *WJO*, vol. 9, no. 4, pp. 60–64, 2018, doi: 10.5312/wjo.v9.i4.60.

[65] R. Gandhi, J. De Beer, D. Petruccelli, and M. Winemaker, "Does patient perception of alignment affect total knee arthroplasty outcome?," Canadian Journal of Surgery, vol. 50, no. 3, pp. 181–186, 2007.

[66] Nakajima , "Association between limb alignment and patient-reported outcomes after total knee arthroplasty using an implant that reproduces anatomical geometry," *J Orthop Surg Res*, vol. 13, no. 1, 2018, doi: 10.1186/s13018-018-1030-8.

[67] K. Wada , "Rotational and varus–valgus laxity affects kinematics of the normal knee: A cadaveric study," *J Orthop Surg (Hong Kong)*, vol. 27, no. 3, p. 230949901987372, 2019, doi: 10.1177/2309499019873726.

[68] A. J. Cyr, S. S. Shalhoub, F. G. Fitzwater, L. A. Ferris, and L. P. Maletsky, "Mapping of Contributions From Collateral Ligaments to Overall Knee Joint Constraint: An Experimental Cadaveric Study," vol. 137, no. 6, 2015, doi: 10.1115/1.4029980.

[69] D. D. D'Lima, B. J. Fregly, S. Patil, N. Steklov, and C. W. Colwell, "Knee joint forces: prediction, measurement, and significance," *Proc Inst Mech Eng H*, vol. 226, no. 2, pp. 95–102, 2012, doi: 10.1177/0954411911433372.

[70] R. B. Martin, David B. Burr, Neil A Sharkey, David P. Fyhrie, *Skeletal Tissue Mechanics*. Springer, 2015, pp. 175–225.

[71] M. M. Ardestani, M. Moazen, E. Maniei, and Z. Jin, "Posterior stabilized versus cruciate retaining total knee arthroplasty designs: Conformity affects the performance reliability of the design over the patient population," *Medical Engineering & Physics*, vol. 37, no. 4, pp. 350–360, 2015, doi: 10.1016/j.medengphy.2015.01.008.

[72] A. J. Cyr and L. P. Maletsky, "Unified quantification of variation in passive knee joint constraint," *Proc Inst Mech Eng H*, vol. 228, no. 5, pp. 494–500, 2014, doi: 10.1177/0954411914530274.